

## Review



**Cite this article:** Crowe CD, Keating CD. 2018

Liquid–liquid phase separation in artificial cells. *Interface Focus* **8**: 20180032.

<http://dx.doi.org/10.1098/rsfs.2018.0032>

Accepted: 11 July 2018

One contribution of 7 to a theme issue

'The artificial cell: biology-inspired compartmentalization of chemical function'.

### Subject Areas:

biomimetics

### Keywords:

synthetic cytoplasm, aqueous two-phase system, coacervate, droplet

### Author for correspondence:

Christine D. Keating

e-mail: [keating@chem.psu.edu](mailto:keating@chem.psu.edu)

# Liquid–liquid phase separation in artificial cells

Charles D. Crowe and Christine D. Keating

Department of Chemistry, Pennsylvania State University, University Park, PA 16802, USA

CDC, 0000-0002-9353-5340; CDK, 0000-0001-6039-1961

Liquid–liquid phase separation (LLPS) in biology is a recently appreciated means of intracellular compartmentalization. Because the mechanisms driving phase separations are grounded in physical interactions, they can be recreated within less complex systems consisting of only a few simple components, to serve as artificial microcompartments. Within these simple systems, the effect of compartmentalization and microenvironments upon biological reactions and processes can be studied. This review will explore several approaches to incorporating LLPS as artificial cytoplasm and in artificial cells, including both segregative and associative phase separation.

## 1. Introduction

Construction of artificial or synthetic cells can lead to advances in understanding cell biology and in other fields such as biotechnology, medicine or materials science where inspiration from biology can be applied in new ways [1–5]. For the purposes of this review, we will use the terms 'artificial' and 'synthetic' interchangeably and consider only artificial cells produced from the bottom-up, by combining biological or non-biological components to produce microscale assemblies that are meant to serve as mimics of one or more aspects of biological cells (e.g. the presence of a semipermeable membrane, and/or the ability to perform a simple reaction). As artificial cells are developed, it is important to bear in mind that the interior of living cells is not uniform, but rather contains many distinct regions and compartments with different composition and physical properties, which can be reflected within the cellular mimics [6]. These range from membrane-bound organelles such as the nucleus and mitochondria to membraneless organelles like the nucleolus. Broadly, organelles serve important functions such as localization, isolation and creation of localized physical microenvironments within the cell interior [6,7]. Many cellular processes rely on these aspects of organelles to house and protect essential components of the cell. For example, in eukaryotic cells, transcription and translation are spatially segregated into the nucleus and cytoplasm, respectively [8]. Within the nucleus, ribosome biogenesis involves three distinct regions of the nucleolus, which is a membraneless organelle [9,10]. In the light of the importance of subcellular organelles in living cells, there has been growing interest in how similar compartmentalization can be achieved in artificial cells.

Membrane-bound and membraneless organelles are both important in cellular compartmentalization and consequently of interest for inclusion within artificial cells. Membrane-bound organelles are surrounded by proteolipid membranes, which separate their interiors from the cytoplasm and control permeability by passive and active transport [7]. Encapsulating smaller lipid vesicles within a larger vesicle provides a simple model for these organelles and has been achieved by several methods [11]. For example, dye-loaded small unilamellar vesicles (SUVs) have been encapsulated during formation of large unilamellar vesicles (LUVs), after which the dye could be released by heating to selectively disrupt the membranes of the SUVs [12]. With recent progress in microfluidics, larger liposomal compartments have been encapsulated within giant lipid vesicles to form 'vesosomes' with controlled size and number of interior vesicles [13].

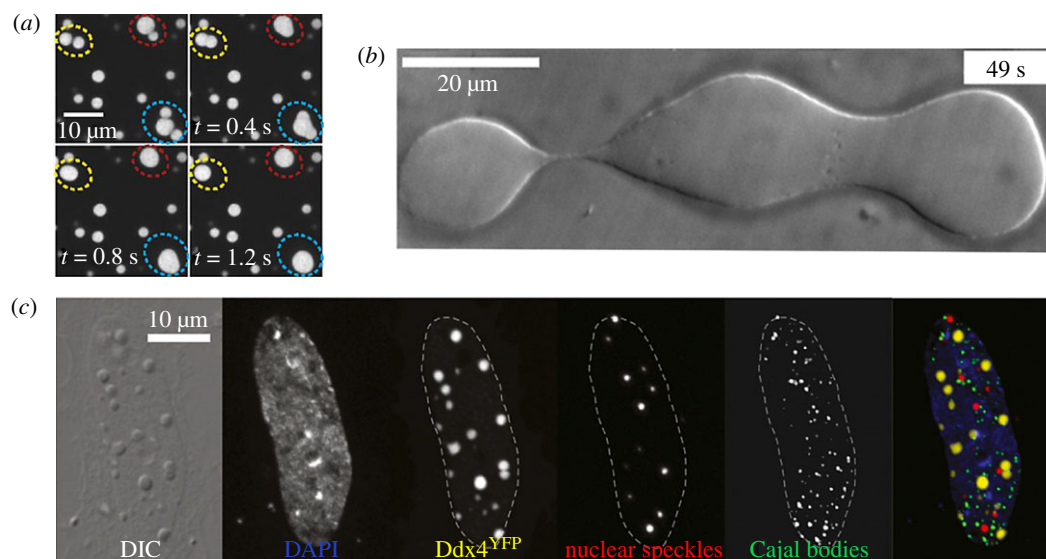


**Figure 1.** Examples of membraneless organelles in living cells. (a) Fluorescence imaging of the protein LAF-1 within P granules show their liquid-like behaviour via coalescence. (b) Coalescence and separation of *X. laevis* nucleoli. (c) Distribution of various membraneless organelles throughout HeLa cell. Images adapted from [24–26]. Image in (c) licensed under Creative Commons (CC BY).

Membraneless organelles include stable, stoichiometric complexes such as the ribosome and the carboxysomes of bacteria [14,15]. Artificial carboxysomes and related structures have been produced as a means of encapsulating multiple copies of enzymes, including sequential enzymes as model pathways [16–18]. Finally, a new class of membraneless organelles has only recently been recognized to form by intracellular liquid–liquid phase separation (LLPS) [19–23]. These ‘liquid organelles’ include the cytoplasmic P granules (figure 1a) [24,27], as well as the nucleolus (figure 1b) [25,26] and nuclear Cajal bodies (figure 1c) [26,28] among others [20]. These behave as liquid-like droplets and demonstrate the ability to merge, split and flow with applied force [27]. A specific example of this is the nucleoli of *Xenopus laevis* oocytes [25]. Brangwynne *et al.* observed these membraneless organelles fusing and separating from neighbouring nucleoli, as seen in figure 1b. Membraneless organelles that form by LLPS in living cells contain proteins and RNA [22,29]. Notably, many of the key protein components have intrinsically disordered regions that are important for organelle formation and for phase separation *in vitro* [30,31]. These organelles, many of which are involved in RNA processing, are dynamic. Their molecular components are able to exchange with the surrounding cytoplasm or nucleoplasm and they can form and dissociate in response to stimuli and/or during the cell cycle. Reversible formation/dissociation and facile exchange of components with the external fluid are useful characteristics for reactive microcompartments and it is thought that intracellular functions can be turned on and off based on reversible localization within membraneless organelles formed by LLPS. For example, sequestration of mRNAs within stress granules halts their translation [32] and assembly of purinosomes, which contain a set of sequential enzymes necessary for de novo purine biosynthesis, is induced by metabolic requirement for purines [33,34].

LLPS is a common phenomenon in aqueous macromolecule solutions and can be achieved using a wide variety of biological or non-biological polymers. It is therefore relatively straightforward to produce synthetic or artificial versions of these intracellular compartments, which can then be used to

explore the consequences of compartmentalization of molecules and reactions. The incorporation of these structures into experimental model systems for cells or cell-like environments is the focus of this review. We will consider four classes of model system that each contain coexisting aqueous phases of distinct composition: (i) ‘bulk’ systems in which droplets of one aqueous phase are dispersed within another continuous aqueous phase (figure 2a); (ii) phase-separated water-in-oil (w/o) emulsion droplets stabilized by surfactants (figure 2b); (iii) lipid vesicle-encapsulated biphasic systems (figure 2c); (iv) Pickering-style emulsions, where lipid vesicles are used to stabilize droplet interfaces against coalescence (figure 2d).

### 1.1. Phase separation in polymer solutions

LLPS is a common physical phenomenon in aqueous polymer solutions. One or more of the resulting phases provides macromolecular crowding due to high concentrations of macromolecules [35,36]. In this way, phase-separated microcompartments are similar to the crowded interior of living cells, which contain high total macromolecule concentrations (e.g. 300–400 mg ml<sup>−1</sup> for *Escherichia coli*) [36–38]. The resulting physical (i.e. excluded volume) and chemical (i.e. preferential interactions) effects can have complex impacts on cellular processes, including influencing reaction rates [39,40] and stabilization of nucleotide secondary structure [41]. As they are able to capture both the crowding and the heterogeneity of intracellular fluids such as the cytoplasm and the nucleoplasm, phase-separated solutions can be useful as models for membraneless organelles. These factors, combined with preferential partitioning of reagents, yield opportunities for exploration of the effects of phase coexistence upon biological reactions and processes [42,43]. We will consider coexisting aqueous phase systems as falling into two broad categories: segregative and associative phase separation, depending on whether the macromolecules are present within separate phases or a single, macromolecular-rich phase, respectively (figure 3a,c) [42,43,46]. In both cases, this process only takes place under appropriate

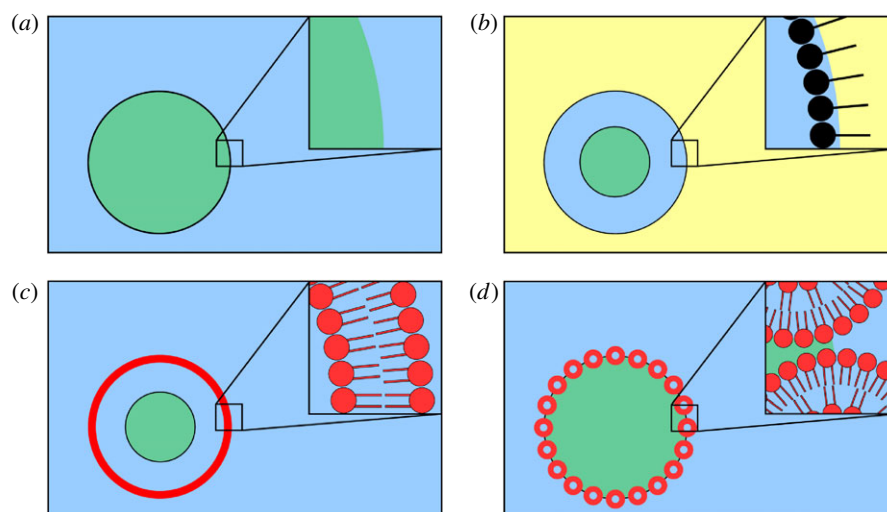


**Figure 2.** Categories of coexisting liquid–liquid systems studied as model cytoplasm for artificial cells. (a) Non-stabilized dispersion of an aqueous phase within another aqueous phase. (b) Surfactant-stabilized w/o emulsion droplets that contain two aqueous phases. (c) Giant lipid vesicles with aqueous phase-separated interiors. (d) Lipid vesicle-stabilized all-aqueous emulsion droplet. In these illustrations, green and blue represent distinct aqueous phases, while yellow indicates oil.

conditions (e.g. concentration, temperature, pH, etc.), resulting in two separate regions containing unique polymer compositions [42,43,47]. These phases are chemically distinct from one another and provide differing solution environments.

### 1.1.1. Segregative phase separation

Segregative phase separation, typically of two neutral polymers or a polymer and a salt, has been used in bioseparations for decades. The components of this system form two regions, each enriched in one of the components (figure 3a depicts segregative solution made using two polymers). Although the phenomenon of phase separation had been explored previously, its most well-known applications in relation to biological systems began in 1955, when Albertsson added polyethylene glycol (PEG) to a solution of chloroplast particles and observed the partitioning of the chloroplasts to a distinct phase [47]. This became a crucial part of the long history of using neutral polymer phase separation as a means of gentle extraction of cellular components [43]. In recent decades, this extensive study of polymer phase separation has led to a deeper understanding of its useful phase behaviour and partitioning characteristics, especially with regard to biomolecules [42,43,48–50]. These aspects of phase-separated solutions (such as biocompatibility and biomolecule partitioning) have led to their use as a valuable tool in the design and exploration of artificial cells intended to host biological reactions without adverse effects.

In the classical example of an aqueous two-phase system (ATPS), the polymers used are dextran (a polyglucose) and PEG [51,52]. Above critical concentrations, a solution of these two polymers phase separates into a dextran-rich and PEG-rich phase (figure 3b). At certain PEG/dextran molecular weights and concentrations, this system is temperature-sensitive, such that phase separation can be induced, for example, by cooling [43,44]. This temperature dependence is shown in figure 3b via the shift of binodal towards lower concentrations of PEG and dextran at lower temperatures [44]. The partitioning preferences of many biological solutes have been reported for many PEG/dextran systems under a variety of conditions [43,53]; this information can serve as a

guide for designing artificial membraneless organelles based on phase coexistence. For example, in general, more hydrophobic solutes such as denatured proteins preferentially accumulate in the PEG-rich phase, whereas more hydrophilic components such as nucleic acids or globular proteins partition into the dextran-rich phase [54,55]. Additionally, biomolecule size is important, as it determines the surface area of interaction with the phase. Larger solutes generally partition more effectively in ATPS; for example, both protein-coated gold nanospheres and RNAs exhibit strongly size-dependent partitioning into the dextran-rich phase of PEG 8 kDa/dextran 10 kDa systems [56,57].

Segregative two-phase systems are also routinely produced using a polymer (such as PEG) and a salt (e.g. citrate, phosphate or sulfate) [42,58]. Here, a hydrophilic salt interacts with the water molecules, leading to a rise in the preferential interactions between polymer molecules. This causes the formation of a polymer-rich phase and a salt-rich phase, similar to the two-polymer system described above. However, the use of different salts in the formation of a polymer-salt solution affects its biomolecule partitioning, causing the selection of salt to be dependent on the intended application [59,60]. Owing to these partitioning characteristics and the low cost of salt compared to polymers such as dextran, these solutions have been used extensively in the extraction of biological materials [61–63].

### 1.1.2. Associative phase separation

The other major method of forming phase-separated systems within artificial cells involves the use of associative phase separation, in which a dense polymer-rich phase (termed a coacervate), and a dilute (polymer-poor) supernatant phase are formed (figure 3c). When oppositely charged polyelectrolytes undergo associative phase separation due to ion-pairing interactions, the process is called complex coacervation [64,65] and has been of particular interest in artificial model systems for membraneless organelles [66–68]. Early examples of complex coacervation started with biologically derived polyelectrolytes, such as a gelatin and gum arabic [69,70]. Here, gelatin (a mixture of proteins) serves as a polycation, while gum arabic (a polysaccharide) functions as the



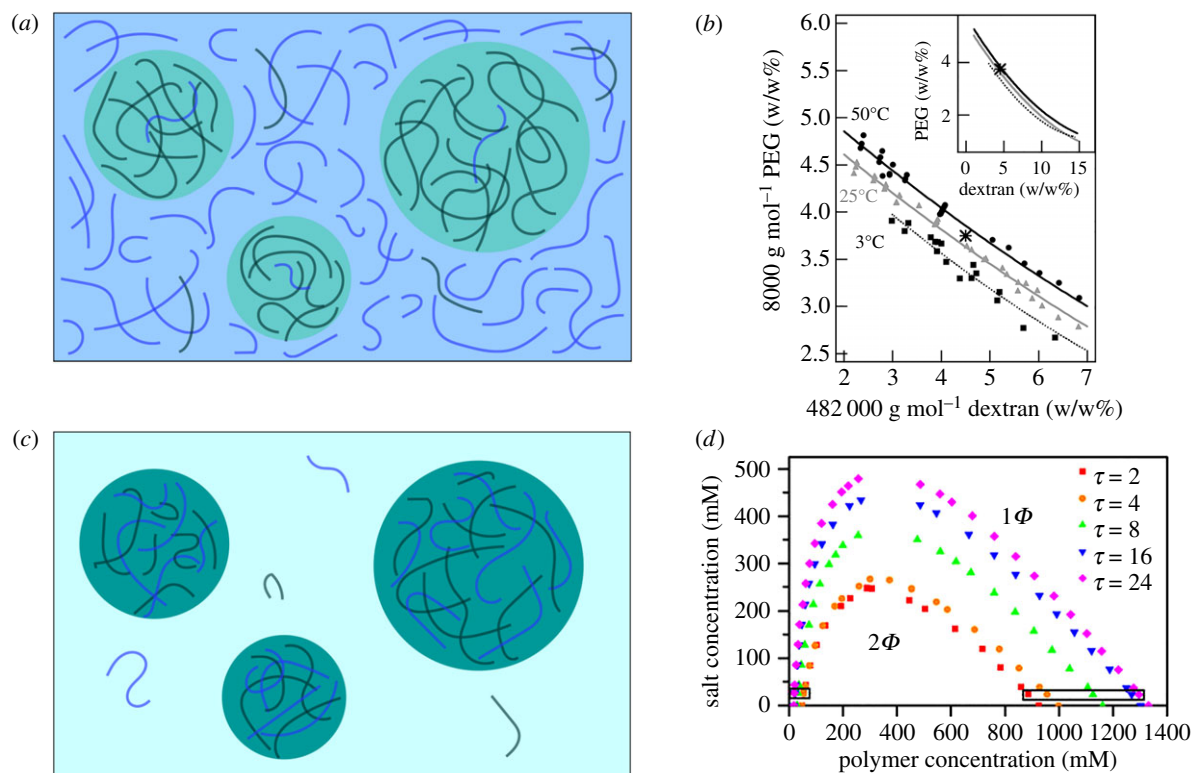


**Figure 3.** Overview of segregative and associative phase separation. (a) Scheme of segregative phase separation of two polymers, where each is primarily localized in one phase. (b) Phase diagram of PEG/dextran ATPS showing phase-transition binodal at varying temperatures. (c) Scheme of associative phase separation of two polymers, where both are distributed within the same, concentrated phase. (d) Simulation of coacervate phase dependence as a function of charge periodicity ( $\tau$ ), salt concentration and polymer concentration. Images adapted from [44,45]. Image in (d) licensed under Creative Commons (CC BY).

polyanion [70]. Biologically derived molecules are still often used to model coacervates, such as the RNA polyuridylic acid (polyU, a polyanion) and the cationic polyamine spermine [67,71,72]. In addition, synthetic polyelectrolytes have also been used. For example, the polyanion polyacrylic acid (PAA) and the polycation polyallylamine hydrochloride (PAH) have been well studied for their coacervation properties [73,74].

Factors influencing the formation and properties of complex coacervates include ion pairing strength, multi-valency, polymer charge density and conformational flexibility, as well as solution ionic strength. Additionally, the ratio of cationic to anionic groups is important, with charge-balanced ratios generally preferred [75,76]. These factors have been explored in both experimental systems and in simulations [45,77]. For example, as seen in figure 3d, simulations predict that as charge periodicity increases, coacervates become more salt-resistant as shown by the size increase in the two-phase region of the phase diagram. If weak polyelectrolytes such as polycarboxylates or polyamines are used, the pH of the system should be tuned such that both polyelectrolyte species are charged [78]. Varying pH can then be used to control formation and dissolution of coacervates [79]. Similarly, the ionic strength of the solution must be considered, as high salt concentration screens the charges between polyelectrolytes, inhibiting the coacervation process or causing dissolution of existing coacervates [73]. The nature of the interaction between salts and polyelectrolytes in the context of complex coacervates is actively being explored [80,81].

Phase separation is often temperature-sensitive, with systems demonstrating upper critical solution temperatures (UCST), lower critical solution temperatures (LCST) or both,

depending on the specific composition [42]. For instance, Quiroz & Chilkoti [82] were able to tune the UCST/LCST behaviour of elastin-like polypeptides by controlling the amino acid repeat sequence and polymer length. Generally, repeat sequences containing more non-polar residues (such as valine) demonstrated LCST behaviour, while those having zwitterionic sequences (such as pairing arginine and aspartic acid) led to UCST behaviour. This could be reinforced by increasing the polymer length (via repeats of the sequence in question), with additional repeats leading to decreased LCST and increased UCST for respective systems.

These sensitivities to solution conditions and polymer composition also provide a method by which the formation and dissolution of the associative phases can be controlled. For example, the addition of salt to a system with complex coacervates can cause the coacervates to dissolve, releasing the polyelectrolytes and partitioned solutes. Similarly, by adjusting the solution temperature either above a UCST or below an LCST (depending on the specific system), the coacervates can be reversibly dissolved. Changing the temperature back into the two-phase region of the phase diagram will lead to reformation of the coacervates.

Associative phase-separated systems with dilute continuous phases can serve as models of prebiotic compartmentalization for the concentration of dilute oligomers. Prebiotic organic oligomers and polymers generated by reactions on the early earth, and especially those having functional capabilities such as catalysis or selective binding, are expected to have been dilute [83–85]. However, the rise of biological reactions necessitates the close proximity of such molecules. Complex coacervation has been proposed as a method to address this. In this theory, dilute

polyelectrolytes of opposite charge would slowly accumulate into coacervate droplets over time, creating a separate phase with locally high concentration where biological reactions may take place [66,86,87]. Artificial cells mimicking such environments are of interest.

## 2. Bulk two-phase systems and water-in-water droplets

Bulk ATPS and coacervate systems have been used as models for biological microcompartments. These systems are often studied as dispersed droplets formed by mechanical agitation of pre-existing phase-separated systems (e.g. vortexing a PEG/dextran ATPS) or by examining systems subsequent to inducing phase separation and prior to coalescence (figure 4a) [90]. Droplets in these systems will eventually coalesce and form macroscopic phases; this process can be aided by centrifugation or resisted by continued agitation of the sample to preserve dispersed droplets. The rate of coalescence, which depends on specific properties of the solution (including surface tension, phase volumes and viscosities), can vary from minutes to hours in different systems.

Well-controlled droplets of one phase of a phase-separated system may be dispersed within the second phase by microfluidics. Microfluidic devices used for this include polydimethylsiloxane (PDMS)-based devices and glass capillary devices [91,92]. Briefly, PDMS-based devices are produced via soft lithography, using PDMS poured over features corresponding to the desired channel dimensions and shape. The PDMS is removed and sealed against a glass surface, resulting in channels that may be used for fluid flow. Glass capillary devices consist of multiple small-radii glass capillaries nested within one another. By controlling the direction and force of flow, droplets may be produced. We refer the interested reader to several comprehensive overviews published on the subject of microfluidic droplet generation, both in general [91,93–95] and focused on phase-separated solutions and aqueous–aqueous systems [96–98].

### 2.1. Partitioning and reactions in bulk two-phase systems

Bulk phase-separated media can serve as a model system for quantitative studies of solute partitioning and its impact on reaction rates and locations. Compartmentalization in the droplet phase of a two-phase system can increase reaction rates by increasing local concentrations. For example, Strulson *et al.* [57] demonstrated rate enhancements for a two-piece ribozyme cleavage reaction in a PEG/dextran ATPS under subsaturating  $k_{\text{cat}}/K_M$  single-turnover conditions, where enzyme concentration is rate-limiting, but not under  $k_{\text{cat}}$  conditions, where the reaction is insensitive to enzyme concentration. These experiments benefited from strong partitioning of the ribozyme into the dextran-rich droplet phase, with a 3000-fold higher concentration in this phase. By varying the relative volumes of the PEG-rich to dextran-rich phases, while holding constant the total ribozyme concentration, total solution volume and crowding conditions, it was possible to observe the effect of local concentration (figure 4b) [57]. Cacace & Keating [99] used a

similar approach to restrict calcium carbonate precipitation to the dextran-rich phase of bulk PEG/dextran ATPS by maintaining a locally higher concentration of the enzyme urease within the dextran-rich phase, such that the mineralization precursor, carbonate, was produced only in this phase. It should be noted that substantial media effects due to the presence of polymeric solutes are generally observed in these systems, such that reaction kinetics in the two phases differ from each other and from reactions in buffer alone. It is generally not possible to predict these media effects and hence quantitative understanding of how compartmentalization impacts rates in multi-phase systems requires separate experimental determinations of reaction kinetics in each phase (done by separating the two phases), as well as local concentrations of all reaction components (enzymes, substrates, products) [88,100]. For example, the ribozyme reaction mentioned above had a higher rate when performed in the PEG-rich phase than in dextran-rich phase or buffer alone, but nonetheless did not occur in the PEG-rich phase when within the ATPS due to its accumulation in the dextran-rich phase [57].

It should not be assumed that reaction rates will increase in a compartmentalized medium. The partitioning of substrates, intermediates, and products, as well as the kinetic performance of each reaction in each phase of the system will influence results. These effects have been explored through experiments and simulations for pairs of sequential enzymes in PEG/dextran and PEG/citrate biphasic systems. By experimentally determining the partitioning of all components and the kinetics for reactions run under the same conditions in each phase alone, it was possible to develop a mathematical model that could predict the concentrations of all species over time in the biphasic systems [88,100]. However, neither case showed strong enhancement of overall reaction kinetics despite co-localization of the sequential enzymes. In the case of purine biosynthetic enzymes corresponding to steps 8 and 9/10 of the *de novo* purine biosynthetic pathway, simulations indicated that more complete partitioning of the enzymes into the droplet phase was needed for increased overall rates [100]. For glucose oxidase and horseradish peroxidase in a PEG/citrate system, preferential accumulation of the amplex red substrate in the PEG-rich phase while the enzymes were co-localized in the citrate-rich phase resulted in interfacial reaction (figure 4c) [88]. This system also showed very poor HRP activity in PEG-rich phase, which can be understood in terms of weak binding between the substrate and the PEG, which is present in high concentrations and effectively sequesters substrate away from the enzyme even in PEG-rich solutions where no phase separation is present [101].

For coacervate systems, where the interior and exterior media are generally even more different in composition and physical properties than in the segregative phase system examples above, the locally high viscosities and high concentrations of potential binding sites (e.g. ion pairing or H-bonding with coacervate polymeric components) can be expected to impact folding and activity of biomolecular solutes. These effects can be expected to depend strongly on the coacervate composition and biomolecule identity. This is an area of current study in the coacervate community, and several interesting examples have already appeared. Nott *et al.* [102] observed helicase activity for protein-based coacervate droplets, in which nucleic acid length and single- versus

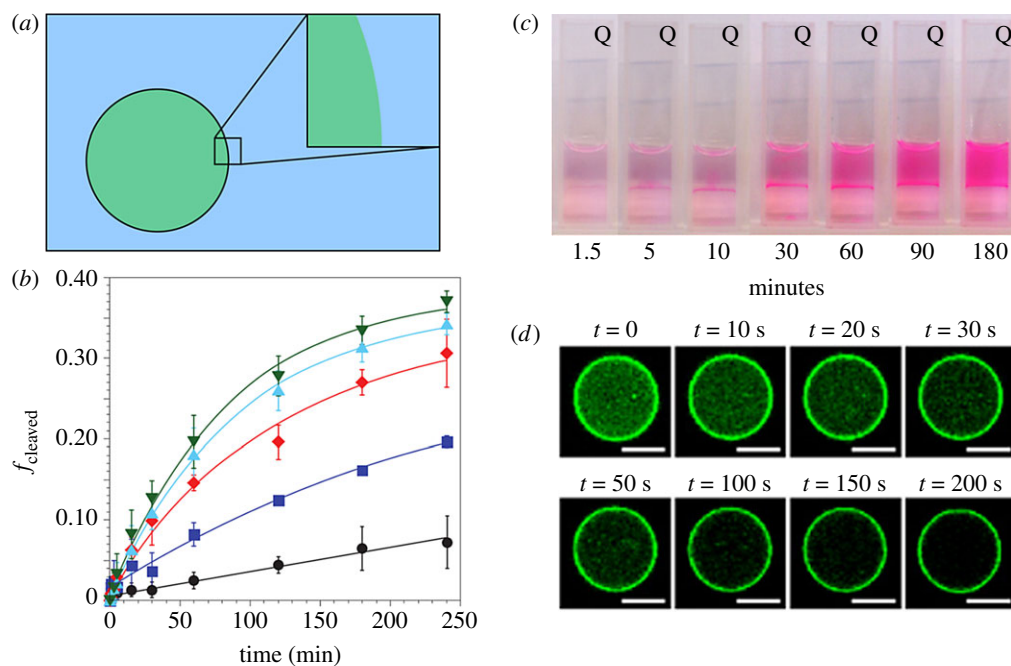


**Figure 4.** Examples of bulk two-phase systems and reactions contained within. (a) Scheme of non-stabilized aqueous phase dispersed within another aqueous phase. (b) Reaction progress of hammerhead ribozyme (HHL) within PEG/dextran ATPS with varying phase volumes. Ratios of PEG : dextran phase volume are 1 : 0 (black circles), 1 : 5 (blue squares), 1 : 12.5 (red diamonds), 1 : 50 (blue triangles) and 1 : 100 (green inverted triangles). (c) Production of resorufin at interface of PEG/citrate ATPS demonstrating interfacial reaction. (d) Release of BSA-FITC from PDDA/PAA coacervate due to unfolding upon addition of urea. Scale bars are 5  $\mu\text{m}$ . Images adapted from [57,88,89]. Image in (d) adapted with permission from [89]. Copyright 2016 American Chemical Society.

double-strandedness was found to be important for partitioning. Sequences that were short or single-stranded were accumulated into the droplets while those with longer persistence length (longer double-stranded sequences) were excluded. The authors ascribe this to a mesh-like coacervate interior that could accommodate only those sequences that were small or flexible enough to pass the mesh [102]. By contrast, Frankel *et al.* [103] saw no dependence on RNA length or sequence for partitioning into PAH/adenosine triphosphate (ATP) coacervates. Here, the mechanism of RNA accumulation appears to be exchange of the ATP coacervate components for the RNA, which has much greater multivalency. As all the RNAs could displace ATP effectively, no sequence or structure dependence was observed. Additionally, the partitioning was extremely strong in these systems, with approximately 100 000-fold greater RNA concentrations inside the coacervates than in the dilute phase. Martin *et al.* [89] recently reported that proteins show folding-dependent partitioning in poly(diallyldimethylammonium)/poly(acrylate) coacervates. In their folded, globular conformations bovine serum albumin (BSA), carbonic anhydrase and  $\alpha$ -chymotrypsin all accumulate within the coacervates. Upon urea-induced unfolding, these proteins are released from the droplets, as seen in figure 4d [89]. The presence of coacervate droplets and the nature of their surface charge was found to play a role in the stepwise renaturation of these proteins [89].

Despite the complexity of these systems, several examples of their ability to support biologically important enzymatic reactions have appeared, including *in vitro* gene expression [104], and activity for the three-enzyme minimal form of actinorhodin polyketide synthase [105]. Additionally, enzymatic reactions have been used to control the formation and dissolution of complex coacervate droplets by changing the phosphorylation state of component molecules in order to change their ability to ion-pair [106,107]. Such approaches

demonstrate a simple mechanism by which post-translational modification of proteins can be used to regulate compartmentalization *in vivo*; phosphorylation state is known to be important in formation of several membraneless organelles [10,108].

## 2.2. Microfluidic droplet generation in all-aqueous systems

Additional control over the production of these phase-separated droplets is desired in order to thoroughly explore the effect of their physical characteristics. This has been accomplished through the use of microfluidics to produce homogeneous, phase-separated droplets [97,98,109]. However, for segregative phase-separated solutions, fluid flow alone is not sufficient to cause separation of the dispersed phase into individual droplets, due to the extremely low interfacial tension between the two phases. The pressure between the two fluids does not provide enough shear force to cause the droplets to pinch. Instead, coflow is much more likely, where the liquids flow alongside each other in distinct streams [96]. This is typically addressed through the introduction of some other physical means of inducing droplet formation, such as piezoelectric bending discs [110,111], mechanical perturbation [112,113] or extremely low flow rates [114]. For instance, Moon *et al.* [114] used hydrostatic pressure to achieve passive production of dextran-rich droplets within a PEG-rich continuous phase. By varying the inlet pressure, they could achieve control over the size of the droplets produced.

Microfluidics has also been used to produce uniform droplets using associative phase-separated systems. Vanswaay *et al.* [115] accomplished this by preparing a bulk coacervate phase of poly(diallyldimethylammonium chloride) (PDDA) and ATP, separating it from the continuous



phase and flowing the two through a flow-focusing PDMS-based device. While this is difficult with segregative phases (as discussed above), the high viscosity of the associative phases induces stretching along the length of the jet, leading to recoil and droplet separation that can be controlled through the flow rate of the two phases [116]. Interestingly, the complex coacervate droplets formed by Vanswaay *et al.* did not coalesce upon contact and were also able to maintain distinct populations of fluorescently tagged DNA oligomers over long times, despite their close proximity. This is in contrast with earlier studies using similar coacervates made without using microfluidics, which displayed exchange of labelled nucleic acid oligonucleotides between coacervate droplets within a population [117]. The ability to resist droplet fusion and diffusive solute exchange is potentially important when considering coacervate droplets as protocell models.

### 3. Phase-separated water-in-oil emulsion droplets

In the previous section, all of the systems discussed contained at least one macroscopic phase. Biological cells are inherently microscale, ranging from 0.5  $\mu\text{L}$  for some oocytes down to less than a femtolitre for certain bacteria [118]. For biomolecules present at relatively low concentrations, the absolute number of molecules, and fluctuations in this number, can become important. Biological cells also have a much higher surface to volume ratio than bulk solutions, making the interactions between cytoplasmic components and membranes more common and more important than those between bulk artificial cytoplasm and the containers that hold them. W/o emulsions can be used to provide individual, diffusion-limited droplets that contain multiple internal phases with microscale total volumes, rendering the system closer to biological cells while at the same time conserving precious reagents (figure 5a).

The oil phase formulations used for these emulsions are varied, ranging from mineral oil [119,120,123] and other hydrocarbons [124,125] to fluorocarbons [121,126,127]. Choosing a specific oil base depends on a variety of factors, including viscosity, density and chemical characteristics. For instance, fluorinated oils are typically used in systems that contain hydrophobic components that would be sufficiently soluble in a hydrocarbon-based oil phase to hamper reactions [94,128]. However, the interfacial tension between the aqueous phases and the oil phases are typically too high to produce stable droplets. Thus, surfactants are required. Surfactant selection is highly dependent upon the specific system, requiring consideration of the potential interactions between the surfactant and the encapsulated reagents. For example, non-ionic surfactants are typically used for encapsulating reactions containing charged species, as an ionic surfactant would interact with these and cause potentially detrimental effects. Because of the wide variety of available oils and surfactants, there is a large library of potential oil phase formulations, although fluorosurfactants are generally reserved for fluorinated oils [94].

Multi-phase w/o droplets can be produced by simply mixing a small volume of aqueous solution with the oil and surfactant (e.g. vortexing). The aqueous solution may already contain coexisting aqueous phases or the phases

can be formed after encapsulation (e.g. by changing the temperature). As an example, a PEG/dextran ATPS will easily emulsify into droplets within a continuous oil phase. More complex systems, e.g. a PEG/dextran/ficoll aqueous three-phase system (A3PS), can also be produced in the same way, as shown in figure 5b [119]. This approach is very simple, but the resulting droplets can be heterogeneous in size and in relative aqueous phase volumes, with some droplets containing all of the phases while others encapsulate only one phase.

Microfluidic droplet generation can provide additional control to produce populations of nearly identical multi-phase w/o droplets. The high interfacial tension between the aqueous and oil phases facilitates droplet formation, allowing for production of monodisperse droplets with controllable features [94,129]. Microfluidic w/o emulsions have been used for many years in a variety of biological applications, including digital droplet polymerase chain reaction (ddPCR) [130,131], protein expression [119,122] and cell sorting [132,133]. In recent years, phase-separated solutions have begun to be used in the microfluidic creation of these emulsions as well, especially those using segregative phase separation, such as PEG/dextran ATPS [96,121,127,132,134]. Lee *et al.* studied the production of PEG/dextran containing droplets within a perfluorodecalin-based oil phase [121]. By controlling the flow rates of the produced droplets and the viscosity of the aqueous phases (via polymer concentration), the mixing of the two phases within the droplet could be influenced. At high flow rates (anywhere from approx. 1  $\text{mm s}^{-1}$  to approx. 10  $\text{mm s}^{-1}$ , depending on fluid viscosity), the dextran-rich phase within the droplets adopted a stretched morphology, as seen in figure 5c. This facilitates control over the interfacial area between the two phases, which is an important component in studying biological processes that have potentially different partitioning behaviour between the two phases.

Protein expression has been studied within ATPS w/o emulsion droplets produced both with and without microfluidics. Torre *et al.* [119] explored the expression of the fluorescent protein mYPet within PEG/dextran ATPS droplets. DNA encoding the protein was added to the ATPS with transcription/translation machinery before being added to a mineral oil phase containing the surfactants Span 80 and Tween 80. When the solution was vortex mixed, the ATPS was dispersed within the oil phase and stabilized by the surfactants. Upon incubation at 37°C, fluorescence microscopy confirmed the production of mYPet, which partitioned into the dextran-rich phase (figure 5d). Similarly, PEG/dextran ATPS has been used to explore the assembly of the bacterial cytoskeletal protein FtsZ, which is essential for cell division [120,123]. Monterroso *et al.* [120] used a mineral oil phase containing dissolved *E. coli* lipids, which acted as a surfactant, as the continuous phase to disperse PEG/dextran droplets within. The lipids assemble at the interface of the droplet, modelling one leaflet of the cellular membrane, the *in vivo* location the FtsZ would typically assemble. Upon production, the FtsZ was observed to bind strongly to the lipid coating, as seen in figure 5e, similar to the behaviour of the protein within the cell. Following this study, Sobrinos-Sanguino *et al.* [123] produced these same droplets using microfluidics, yielding a monodisperse population of lipid-stabilized, FtsZ-containing droplets in oil.

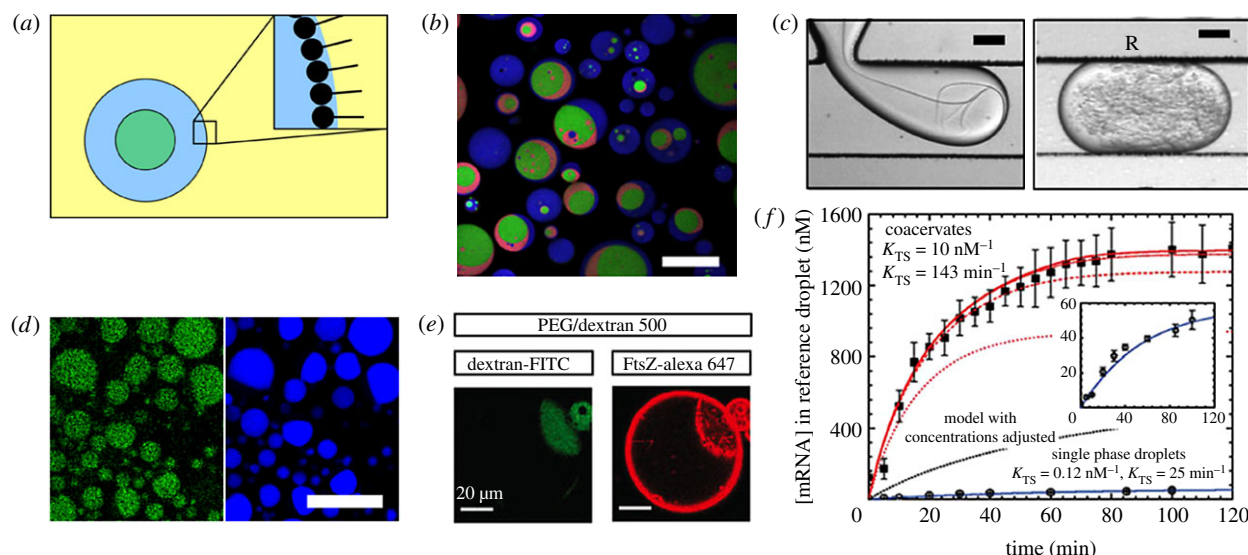


**Figure 5.** Examples of phase-separated w/o emulsion droplets stabilized via surfactant and their use as artificial cells. (a) Scheme of surfactant-stabilized w/o emulsion droplet containing a phase-separated solution. (b) Aqueous three-phase system w/o emulsion droplets containing PEG (blue), dextran (green) and ficoll (red). Scale bar is 50  $\mu\text{m}$ . (c) Microfluidic production of PEG/dextran droplet within an oil phase showing control over internal aqueous mixing via flow rate. Scale bar is 100  $\mu\text{m}$ . (d) Production of mYPet (green) within phase-separated droplets containing PEG and dextran (blue). Scale bar is 25  $\mu\text{m}$ . (e) Assembly of produced FtsZ within dextran-rich phase and at lipid-coated interface of PEG/dextran droplets. (f) Increase in transcription rate when carried out within coacervate droplets compared to a single-phase solution. Images adapted from [119–122]. Image in (f) licensed under Creative Commons (CC BY).

Sokolova *et al.* [122] used a microfluidic platform to produce w/o emulsion droplets with coexisting phases comprised *E. coli* cell lysate and PEG. Phase separation was achieved through dehydration of initially single-phase droplets containing cell lysate and PEG surrounded by a fluorinated oil phase. The droplets are immobilized in recessed wells, where they are in contact with a 15  $\mu\text{m}$  PDMS membrane separating them from a constant flow of saturated salt solution. This induces osmotic dehydration of the droplets, reducing their volume and increasing the concentration of the cell lysate and PEG such that phase separation was induced. After developing this method of coacervate production, protein expression was carried out within the droplets, using a molecular beacon to observe mRNA production and the final product's fluorescence (green fluorescent protein). The transcription rates were found to be increased by a factor of 50 when compared with single-phase droplets (figure 5f).

Segregative and associative systems have been incorporated in w/o emulsion droplets and have been demonstrated to support biologically relevant reactions within them. However, the requirement of (typically) non-biological surfactants can limit their applicability to all systems, as this introduces an additional component with which the system of study can interact [94,128]. Often, these interactions are detrimental, such as causing protein adsorption at the droplet interface or denaturation [135,136]. Additionally, the presence of a large, non-polar continuous phase can cause issues with non-polar reagents. Typically, any required reaction materials will partition almost exclusively to the aqueous interior of the droplets. However, non-polar additives may be likely to dissolve into the oil phase, where it will be diluted and effectively unavailable for participation in reactions otherwise contained within the droplets. While these factors can limit the design of multi-phase w/o emulsions in artificial cells, these issues can typically be addressed by careful selection of the oil and surfactant used.

## 4. Phase separation in giant vesicles

Cell-sized or 'giant' vesicles (GVs) with uniform interiors are often used as models for cellular membranes in artificial cells [44,137–141]. In the ideal case, the GV membrane is only one bilayer of phospholipids, creating a giant unilamellar vesicle (GUV) (figure 6a). PEG/dextran ATPS have been encapsulated within GV by gentle hydration and electroformation to form model cells that contain crowded, phase-separated aqueous interiors [44,137,142]. Gentle hydration is a traditional method for producing GV [141,145]. In this process, lipids are dissolved in an organic solvent before being dried on the surface of a container. Following this, the aqueous solution that is to be encapsulated is introduced. As the aqueous solution hydrates the lipid film, it peels off of the walls of the container, forming a variety of different structures, including GV that are multi-lamellar and GUVs. Electroformation is also commonly used for vesicle production, and can give improved yields of unilamellar vesicles [143,145,146]. In this process, lipid hydration and liposome formation occur on the surface of electrodes due to application of an electric field. The parameters of the electric field depend on the specific mix of lipids used, as well as the solution chemistry [145,146]. Incorporation of coexisting aqueous phases within vesicles prepared by either of these methods is performed by ensuring that the solution exists as a single phase during vesicle formation, by elevated temperature or reduced polymer concentration, for example. Phase-separation is subsequently induced by cooling and/or osmotic concentration of vesicle contents (figure 6b) [44,51,142,147,148].

Long *et al.* [142] reported yields for vesicles that contained both phases of about 50%, with about 40% of these being GUVs, while the rest had additional lipid lamella. These values were surprisingly high, given the poor encapsulation efficiency of macromolecules in vesicles prepared by gentle hydration and the fact that polymer concentrations used during vesicle growth were very close to the



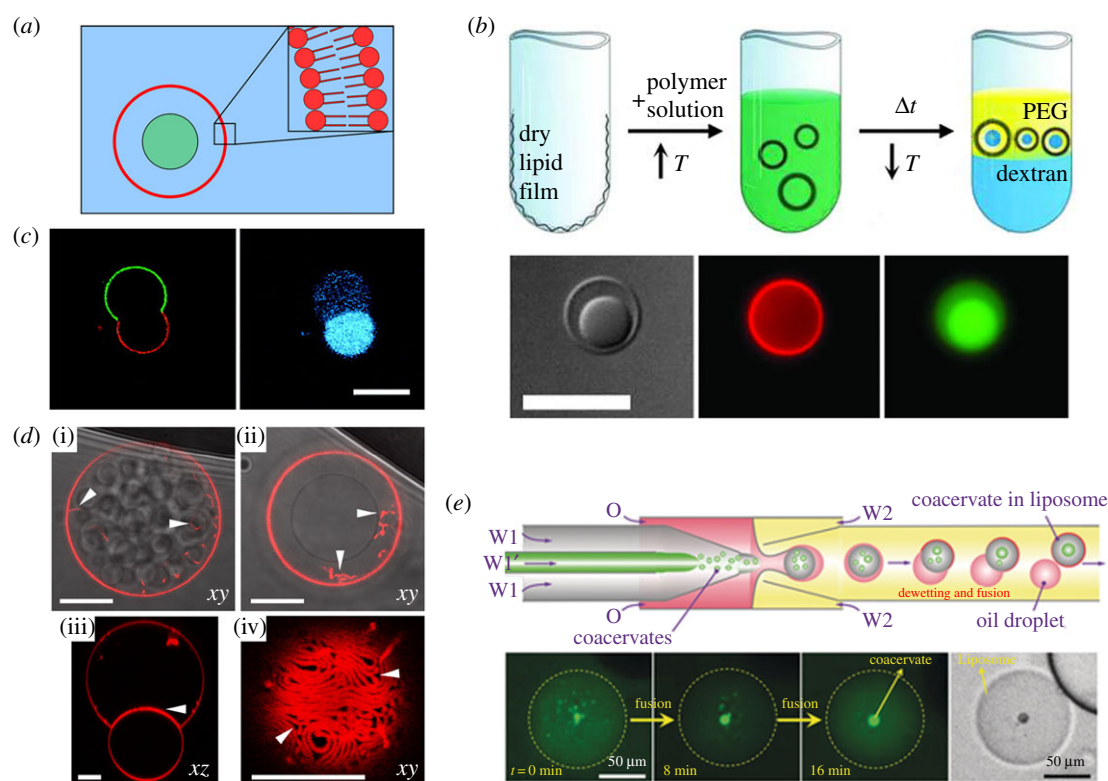


**Figure 6.** Examples of phase-separated GV as artificial cells. (a) Scheme of GV containing a phase-separated solution. (b) Overview of gentle hydration of lipid film with a PEG/dextran ATPS. Bottom shows final droplet with lipid membrane (red) surrounding phases of PEG and dextran (green). Scale bar is 10  $\mu\text{m}$ . (c) Osmotically induced budding of lipid-coated ATPS droplets. Separate lipid domains of PEGylated lipids (green) and non-PEGylated lipids (red) surround the PEG-rich and dextran-rich phases, respectively. A protein, soyabean agglutinin (blue), partitions into the dextran-rich phase. Scale bar is 10  $\mu\text{m}$ . (d(i,ii)) Osmotically induced shrinkage of PEG/dextran droplets causes phase separation and formation of lipid nanotubes (red with arrowheads). (iii) xz view of droplet shows lipid nanotubes at aqueous-aqueous interface. (iv) Image from arrowhead in (iii) shows lipid nanotubes at interface. All scale bars are 15  $\mu\text{m}$ . (e) Scheme of coacervate-containing liposome production via microfluidics. Bottom shows fusion of polylysine/ATP coacervates after droplet formation. Images adapted from [71,142–144]. Image in (b) Copyright (2005) National Academy of Sciences. Image in (e) licensed under Creative Commons (CC BY).

coexistence curve, such that modest dilution would render the system unable to phase separate even at low temperature. Further studies on polymer encapsulation demonstrated that although at low concentrations, large macromolecules such as dextran 500 kDa are very poorly encapsulated, addition of higher total polymer concentrations (e.g. 3 wt/wt% PEG or dextran) resulted in crowding-induced polymer condensation [149,150]. This increased the encapsulation amounts and vesicle-to-vesicle uniformity for the polymers themselves [149] and for various included biomolecules, such as fibrinogen and ssDNA [150].

Encapsulated proteins could be compartmentalized by partitioning into one of the phases or released throughout the artificial cell interior by undergoing a thermal phase transition such that the interior volume was mixed or phase-separated [142]. Changes in protein distribution between the intracellular compartments could be induced by changing the protein conformation. Dominak *et al.* [151] demonstrated that acid- or base-denatured proteins accumulated in the PEG-rich phase of PEG/dextran ATPS-containing GV, while the native globular form of these proteins partitioned into the dextran-rich phase. Changes in the external pH could be used to induce protein conformational changes and re-localization between the phases.

The lipid bilayer is permeable to water but not osmolytes such as sucrose or glucose; hence, the interior volume of the GV can be controlled via the concentration of osmolytes in the external solution. When GV containing phase-separated

solutions are placed under osmotic pressure, they begin to shrink. This concentrates the encapsulated polymers, increasing the interfacial tension at the aqueous/aqueous boundary between encapsulated phases, while at the same time providing excess membrane area. Together, these effects drive GV budding, which minimizes the contact area between the interior phases [152,153]. In the resulting budded structures, the 'bud' and 'body' regions of the GV contain different polymer-rich phases, complete with partitioned solutes, such as proteins [152]. When coexisting lipid phase domains are also present, interactions between the lipid headgroups and the interior phases determine the wetting of the two-dimensional lipid phase domains on the three-dimensional interior aqueous domains. For instance, when PEGylated lipids are present at higher concentration in the liquid-ordered membrane domains, these domains preferentially wet the PEG-rich interior phase of PEG/dextran droplets, leaving the non-PEGylated lipids to wet the dextran-rich phase [154]. This was visualized by Andes-Koback & Keating through the inclusion of fluorescently labelled soyabean agglutinin, which accumulated within the dextran-rich phase of the budded droplet surrounded by the non-PEGylated lipid domain (figure 6c). In this way, simple artificial cells can be produced in which both the interior cytoplasm mimic and the encapsulating membrane are polarized, with different molecular composition at the two ends of the budded vesicle structure. Further osmotic deflation can lead to complete budding and enable asymmetric fission of

droplets, with one daughter vesicle containing the PEG-rich phase surrounded by PEGylated lipids and the other with the dextran-rich phase surrounded by non-PEGylated lipids [144]. As before, the daughter droplets maintain the partitioning behaviour of the original GV. This mimics via simple physical–chemical principles the asymmetric division of living cells [155,156]. While extant cells have complex and highly evolved systems for controlling division that rely on many specific proteins, the general concept of asymmetric fission would have been important early in cellular history and studies such as these using only very simple components can point to potential mechanisms for protocell division.

The osmotic manipulation of these GVs has also been used in the production of internal lipid structures within phase-separated droplets. Li *et al.* created droplets of a single-phase PEG/dextran solution within lipid vesicles produced via electroformation [157]. Upon addition of a hypertonic sucrose solution, the vesicles deflated, shrinking the droplet volume and inducing phase separation (in progress in figure 6*d*(i), complete in figure 6*d*(ii)). With the resulting excess membrane surface area/vesicle volume, lipid nanotubes formed and extended into the interior of the vesicle, as marked by arrowheads in figure 6*d*(i,ii). These nanotubes assembled at the interface between the PEG-rich and dextran-rich phases, forming a mesh of lipid nanotubes (figure 6*d*(iii,iv)). As additional nanotubes formed beyond the capacity of the aqueous/aqueous interface, they began reaching vertically into the PEG-rich phase. The formation of these lipid nanotubes from the surface lipid membranes of a phase-separated system has been studied extensively by Dimova & Lipowsky [148,158]. Additionally, the wetting characteristics of the surface membrane has been explored, where the increase in total polymer concentration leads to changes in the wetting behaviour of the interior aqueous phases with the surrounding lipid membrane [147]. The inherent contact angle at the point where the PEG-rich phase, dextran-rich phase and continuous phase meet was found to be a material parameter of the droplet (i.e. dependent on polymer composition and not droplet morphology) [159].

Combining phase-separated interiors with microfluidic vesicle generation is an important step towards production of homogeneous populations of compartmentalized artificial cells with interior compartments that are uniform in both composition and relative volumes [160,161]. This has been done via a w/o-in-water double emulsion approach [71,162,163]. In such systems, the intermediate oil phase contains dissolved phospholipids. After the droplets are formed, the oil phase is removed, leaving the dissolved phospholipids to assemble at the aqueous–aqueous interface. This occurs either by evaporation of volatile organic components, such as toluene and chloroform [71,163], or by the physical removal of the oil phase as the vesicles flow through the device [162]. This process leaves liposome-enclosed aqueous droplets contained within an aqueous continuous phase. Deng & Huck [71] produced coacervate-containing GUVs by first forming a stream of very small coacervate droplets via flowing a solution of polylysine into an ATP solution. This was then passed through an oil phase with dissolved phospholipids before finally meeting an additional aqueous phase. The coacervates within the droplets coalesced while the oil phase de-wet the droplets, leaving a liposome coating. This resulted in a monodisperse population of aqueous

liposomes, each of which contained a nearly identical coacervate droplet (this process is shown in figure 6*e*) [71]. These individual artificial cells could be manipulated in the same way that larger, non-encapsulated coacervates could be, including controlled release and storage of DNA through temperature-induced dissolution and reformation. Transcription was also carried out within these phase-separated structures, as previously explored in other systems [71]. This method of producing lipid-encapsulated droplets with individual coacervates represents a means of creating artificial cells with multiple aspects of mimicry, including phase separation, phospholipid bilayer and controllable reaction dynamics.

While the use of GVs as a means of encapsulation of phase-separated solutions represents the inclusion of an additional critical feature of living cells in cellular mimics, the reliable and uniform production of these droplets remains non-trivial. Although gentle hydration and electroformation are easily implemented within the laboratory setting, the GVs produced are heterogeneous. Microfluidic approaches address this by creating uniform GVs with controllable content, but require fabrication of the microfluidic device itself, as well as the introduction of additional components such as a possibly incompatible oil phase. Continuing advances in encapsulation strategies will benefit the production and study of increasingly complex artificial cells.

## 5. Lipid vesicle stabilization of phase-separated droplets

Although lipid bilayer membranes are an important step towards faithful mimics of biological cells, these structures pose certain challenges in artificial cell production and functionality. For example, it can be challenging to produce monodisperse populations of GVs with predetermined and uniform contents, particularly when this interior volume consists of concentrated, complex mixtures of macromolecules. Once formed, the lipid bilayer membrane is impermeable to most solutes, complicating the use of GVs for reactions in which substrate entry and product egress from the artificial cell is needed. To address these challenges, liposome-stabilized all-aqueous emulsion droplets have been introduced. These structures are Pickering-type emulsions in which large unilamellar lipid vesicles (LUVs, approx. 100 nm in diameter) are used to stabilize the aqueous–aqueous interface, preventing droplet coalescence without serving as a barrier to entry/egress of molecules up to the size of proteins or nucleic acids (figure 7*a*).

The interface-stabilizing LUVs (or SUVs) are prepared by lipid hydration in an osmotically matched solution, extrusion through a membrane to produce the desired vesicle size, and then addition to a phase-separated solution [145]. The lipid vesicles assemble at the interface between the aqueous phases, stabilizing the smaller volume dispersed phase within the larger continuous phase. For example, figure 7*b* shows rhodamine-labelled vesicles (in red) assembled at the interface between an interior dextran-rich phase (labelled green) and an external PEG-rich phase, explored by Dewey *et al.* [164]. Owing to very low solubility of the PEGylated, negatively charged LUVs in both phases of the ATPS, it was possible to control droplet size by changing the number of vesicles added. The addition of more liposomes

led to smaller droplets due to the ability to stabilize more interfacial area between the two phases. Interfacial area stabilized per liposome was greater than could be explained by a close-packed monolayer of LUVs, indicating that the vesicle corona was a submonolayer. Increasing ionic strength resulted in higher LUV packing density due to screening of electrostatic repulsions between LUVs, and reduced the availability of the lipids to stabilize the interface, leading to larger droplets and eventually destabilization [164]. Interestingly, fluorescence recovery after photobleaching (FRAP) experiments demonstrated that the lipid vesicles at the interface of these droplets do not freely diffuse on the surface of the droplets [67,164]. This has been observed in Pickering emulsions, where the high density of individual particles (or vesicles, in this case) does not allow for motion past one another [165]. Here, jamming appears to be due to the electrostatic repulsions between interfacial LUVs rather than to their absolute packing density. Dynamic light scattering measurements show constant liposome size after release of LUVs by phase dissolution, indicating that the liposomes do not undergo coalescence or formation of lipid aggregates while at the interface.

The permeability of the liposome coating can be taken advantage of to incorporate relevant biomolecules within the droplets after their formation. For instance, when DNA within a PEG-rich solution is added to a solution of liposome-stabilized dextran-rich droplets, the DNA diffuses into the droplets, where it accumulates due to its strong partitioning into this phase [164]. Reactions can be initiated within droplets after their formation by addition of reagents or biocatalysts to the external solution [138,164]. For example, a hammerhead ribozyme cleavage reaction was explored by Dewey *et al.* [164] within this system using Förster resonance energy transfer. The presence of the liposome coating was found to have essentially no effect on the reaction rate, despite initiating the reaction through the addition of RNA to the continuous phase, from which it passes the liposome layer to enter the dextran-rich phase for reaction. These structures have also been used as artificial mineralizing vesicles for biomimetic mineralization where post-formation addition of reagents was again used [138]. Specifically, the production of solid calcium carbonate ( $\text{CaCO}_3$ ) within droplets has been accomplished by harnessing the partitioning behaviour of the PEG/dextran ATPs. Solid  $\text{CaCO}_3$  is formed upon the hydrolysis of urea by urease, which produces the carbonate anion ( $\text{CO}_3^{2-}$ ), in the presence of calcium ( $\text{Ca}^{2+}$ ). Mineralization was restricted to the interior, dextran-rich phase due to preferential urease partitioning to this phase, such that when the reaction was initiated by adding urea to the continuous phase, carbonate was produced locally within the LUV-coated droplets [138]. The small molecule chelator ethylenediamine disuccinic acid (EDDS) was used as a  $\text{Ca}^{2+}$  concentration buffer. EDDS had intermediate binding affinity for  $\text{Ca}^{2+}$ , preventing destabilizing interactions between  $\text{Ca}^{2+}$  and the LUV lipid headgroups while allowing  $\text{CaCO}_3$  precipitation. The  $\text{CaCO}_3$  that forms is contained within the droplets, as shown in figure 7c, and can be released for further analysis by diluting the system with water or buffer to dissolve the phases and release the liposomes [138].

Complex coacervates formed from RNA (polyuridylic acid) and polyamines (spermine and spermidine) have also been coated with LUVs [67]. In addition to exploring the physical properties and compartmentalization of these

coacervate droplets, this study also prepared RNA-based coacervates before adding SUVs (approx. 90 nm diameter) as described above. The SUVs assembled at the interface of the coacervate droplets and the continuous phase, as seen in figure 7d. Similar to the segregative phase systems described above, FRAP showed that the vesicles were not mobile. It must be noted, however, that the addition of charged components (such as the polyelectrolytes within a complex coacervate) can have detrimental effects upon the ability of lipid vesicles to stabilize droplets. The presence of excess positively charged spermine within the RNA-based coacervates described above caused a decrease in the effectiveness of the SUV coating to prevent coacervate droplet coalescence [67]. This is likely to be due to the polycation interacting with the negatively charged lipid vesicles, reducing the electrostatic component of their stabilization, similar to the effect of free  $\text{Ca}^{2+}$  in biomineralization trials [138]. Despite the reduced stability of these structures, they nonetheless provide a permeable, lipid membrane-like coating on the crowded coacervate interior. Additionally, the ease with which lipid assemblies accumulate at the aqueous/aqueous interface of segregative or associative phase systems suggests that the surfaces of intracellular membraneless organelles could be expected to be sites for self-assembly of lipid structures or other particulates. The designation of intracellular organelles as ‘membraneless’ is sometimes determined by their ability to exchange contents with the external environment, indicating the absence of an intact bilayer membrane. However, this could still be consistent with the presence of self-assembled particulates that do not impose limits on permeability [166–168].

The general process of using molecular self-assembly of lipids at phase-separated aqueous–aqueous interfaces has also been previously explored through the use of the fatty acids [169]. Tang *et al.* [169] described the formation of oleic acid-based membranes around RNA/protein coacervates through the addition of sodium oleate. Upon introduction, lipid-soluble dye within the coacervate droplets localized at the surface, indicating the formation of an oleic acid membrane. SAXS experiments and fluorescence imaging indicated that the membrane that formed at the coacervate interface was multi-lamellar. Notably, the concentration of sodium oleate added was below its critical micelle concentration, indicating that the formation of the self-assembly was due to the presence of the coacervates and not the oleic acid itself. Although the membrane within this system is not a single bilayer, it is unbroken, semipermeable and negatively charged. These structures could be a stepping-stone to protocell formation in a prebiotic scenario where coacervate droplets serve to compartmentalize organic molecules and the semipermeable lipid coating provides a primitive version of a cell membrane.

## 6. Conclusion

Combining aqueous/aqueous phase separation within artificial cells gives researchers a great many opportunities to manipulate the chemical and physical aspects of biological mimics. Recent developments in this field have worked towards experimentally capturing simpler versions of the various forms of phase separation found within living systems, including the use of both segregative and associative phase



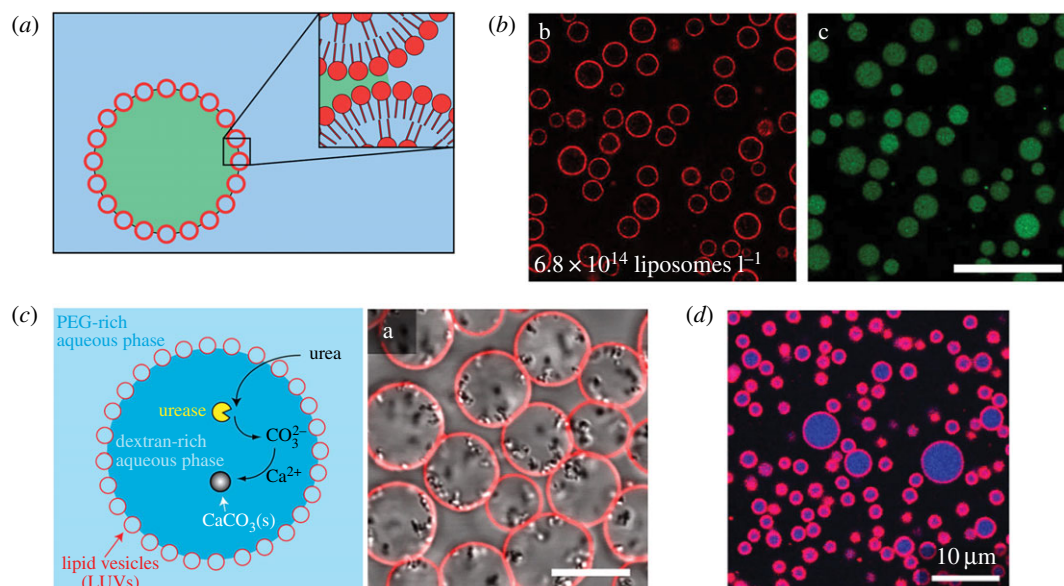


**Figure 7.** Examples of liposome-stabilized Pickering emulsions of phase-separated droplets. (a) Scheme of liposome stabilization of dispersed aqueous phase within continuous aqueous phase. (b) Phase-separated droplets of dextran-rich phase (green) within PEG-rich phase, stabilized by liposomes (red). Scale bar is 25  $\mu\text{m}$ . (c) Cartoon of biomineralization within liposome-stabilized droplets. Right is image of mineral formation within droplets surrounded by liposomes (red). Scale bar is 10  $\mu\text{m}$ . (d) Liposome (red) assembly around coacervate droplets comprised spermine and polyU (blue). Images adapted from [67,138,164]. Image in (c) reprinted with permission from [138]. Copyright 2015 American Chemical Society.

separation. The aspects of these systems that make them beneficial within the cell, such as passive localization and increased local concentration, have been experimentally replicated within these mimics and used to facilitate biological reactions.

However, more work is currently underway to further expand the field of phase-separated artificial cells and to combine these methods of forming phase-separated artificial cells with other existing models of cellular structure and function. For instance, recent work has explored the combination of associative phase separation within crowded solutions, more accurately recreating the environment under which coacervation may occur within cells [72]. The characteristics of polyuridylic acid/spermine coacervates were found to be dependent upon both the presence of macromolecular crowding and the identity of the crowding agent. Additional exploration is being undertaken in the effort to mimic the membranes [3,170,171], chemical pathways [172–174] and replication of living cells [175–178], as well.

To date, the LLPS systems used in cellular mimics have largely been chosen for ease of incorporation. For example, systems able to undergo a phase transition can be encapsulated within vesicles or droplets more easily and hence are overrepresented in this literature. Looking forward, it is additionally becoming apparent that the chemical make-up of the LLPS systems plays an important role in the physical, chemical and biochemical properties of these compartments. Non-biological polymers (such as PEG, polyallylamine and PAA, for instance) have long been used in phase separation studies; however, biopolymers such as proteins and nucleic acids can be used as well. Much effort is currently underway in order to better understand the effects of the chemical natures of these molecules (such as the length, charge density, and periodicity of biological or non-biological polyelectrolytes, or the amino acid sequence of intrinsically disordered proteins) [45,87,179]. As more is learned about the

relationship between chemical structure and phase properties (e.g. polarity, viscosity, partitioning characteristics, crowding, etc.), molecular components can be chosen on the basis of their desired properties for a particular type of cellular mimic.

Microfluidics provides a powerful tool to help address persistent issues with multi-phase artificial cell production, such as polydispersity of droplet populations and lack of control over droplet morphology (e.g. relative phase volumes). Recent developments have expanded the capabilities of microfluidic techniques with respect to biomimicry and biocompatibility, such as their use in the formation of lipid membranes around droplets [71,162,163]. However, it must be considered that microfluidics requires specialized materials and techniques, presenting a barrier to newcomers in mastering these approaches. Once operational, though, microfluidics gives the opportunity for fast and efficient experimentation with artificial cells and offers tremendous promise for continued advances in artificial cell complexity and functionality.

The use of lipid vesicles in the stabilization of phase-separated artificial cells represents a middle ground between faithful reproduction of cellular properties and control over fabrication. These systems exhibit many of the characteristics of a true phospholipid bilayer, such as semipermeability, negative charge and prevention of coalescence. However, they can be created without the risk of heterogeneous coatings or aggregates, as well as without requiring microfluidics. Because of this, phase-separated lipid-stabilized systems function as an appealing template upon which to structure the study of artificial cells.

**Data accessibility.** This article has no additional data.

**Competing interests.** We declare we have no competing interests.

**Funding.** This work was supported by the National Science Foundation (MCB-1715984) and the Department of Energy, Basic Energy Sciences Biomolecular Materials (DE-SC0008633).

## References

- Salehi-Reyhani A, Ces O, Elani Y. 2017 Artificial cell mimics as simplified models for the study of cell biology. *Exp. Biol. Med.* **242**, 1309–1317. (doi:10.1177/1535370217711441)
- Buddingh' BC, Van Hest JCM. 2017 Artificial cells: synthetic compartments with life-like functionality and adaptivity. *Acc. Chem. Res.* **50**, 769–777. (doi:10.1021/acs.accounts.6b00512)
- Spoelstra WK, Deshpande S, Dekker C. 2018 Tailoring the appearance: what will synthetic cells look like? *Curr. Opin. Biotechnol.* **51**, 47–56. (doi:10.1016/j.copbio.2017.11.005)
- Hammer DA, Kamat NP. 2012 Towards an artificial cell. *FEBS Lett.* **586**, 2882–2890. (doi:10.1016/j.febslet.2012.07.044)
- Li M, Huang X, Tang D, Mann S, Luisi PL, Stano P, Chiarabelli C. 2014 Synthetic cellularity based on non-lipid micro-compartments and protocell models. *Curr. Opin. Chem. Biol.* **22**, 1–11. (doi:10.1016/j.cbpa.2014.05.018)
- Gabaldón T, Pittis AA. 2015 Origin and evolution of metabolic sub-cellular compartmentalization in eukaryotes. *Biochimie* **119**, 262–268. (doi:10.1016/j.biochi.2015.03.021)
- Heald R, Cohen-Fix O. 2014 Morphology and function of membrane-bound organelles. *Curr. Opin. Cell Biol.* **26**, 79–86. (doi:10.1016/j.cob.2013.10.006)
- Berg JM, Tymoczko JL, Stryer L. 2012 Transcription in eukaryotes is highly regulated. In *Biochemistry*, pp. 864–869. New York, NY: W.H. Freeman.
- Boisvert FM, Van Koningsbruggen S, Navascués J, Lamond AI. 2007 The multifunctional nucleolus. *Nat. Rev. Mol. Cell Biol.* **8**, 574–585. (doi:10.1038/nrm2184)
- Sirri V, Urcuqui-Inchima S, Roussel P, Hernandez-Verdun D. 2008 Nucleolus: the fascinating nuclear body. *Histochem. Cell Biol.* **129**, 13–31. (doi:10.1007/s00418-007-0359-6)
- Trantidou T, Friddin M, Elani Y, Brooks NJ, Law R V, Seddon JM, Ces O. 2017 Engineering compartmentalized biomimetic micro- and nanocontainers. *ACS Nano* **11**, 6549–6565. (doi:10.1021/acsnano.7b03245)
- Bolinger PY, Stamou D, Vogel H. 2004 Integrated nanoreactor systems: triggering the release and mixing of compounds inside single vesicles. *J. Am. Chem. Soc.* **126**, 8594–8595. (doi:10.1021/ja049023u)
- Deng N-N, Yelleswarapu M, Zheng L, Huck WTS. 2017 Microfluidic assembly of monodisperse vesosomes as artificial cell models. *J. Am. Chem. Soc.* **139**, 587–590. (doi:10.1021/jacs.6b10977)
- Kerfeld CA, Heinhorst S, Cannon GC. 2010 Bacterial microcompartments. *Annu. Rev. Microbiol.* **64**, 391–408. (doi:10.1146/annurev.micro.112408.134211)
- Kerfeld CA, Aussignargues C, Zarzycki J, Cai F, Sutter M. 2018 Bacterial microcompartments. *Nat. Rev. Microbiol.* **16**, 277–290. (doi:10.1038/nrmicro.2018.10)
- Frey R, Mantri S, Rocca M, Hilvert D. 2016 Bottom-up construction of a primordial carboxysome mimic. *J. Am. Chem. Soc.* **138**, 10 072–10 075. (doi:10.1021/jacs.6b04744)
- Godoy-Gallardo M, York-Duran MJ, Hosta-Rigau L. 2018 Recent progress in micro/nanoreactors toward the creation of artificial organelles. *Adv. Healthc. Mater.* **7**, 1700917. (doi:10.1002/adhm.201700917)
- Schoonen L, Van Hest JCM. 2016 Compartmentalization approaches in soft matter science: from nanoreactor development to organelle mimics. *Adv. Mater.* **28**, 1109–1128. (doi:10.1002/adma.201502389)
- Hyman AA, Weber CA, Jülicher F. 2014 Liquid–liquid phase separation in biology. *Annu. Rev. Cell Dev. Biol.* **30**, 39–58. (doi:10.1146/annurev-cellbio-100913-013325)
- Mitrea DM, Kriwacki RW. 2016 Phase separation in biology; functional organization of a higher order. *Cell Commun. Signal.* **14**, 1–21. (doi:10.1186/s12964-015-0125-7)
- Alberti S. 2017 Phase separation in biology. *Curr. Biol.* **27**, R1097–R1102. (doi:10.1016/j.cub.2017.08.069)
- Brangwynne CP. 2013 Phase transitions and size scaling of membrane-less organelles. *J. Cell Biol.* **203**, 875–881. (doi:10.1083/jcb.201308087)
- Wheeler RJ, Hyman AA. 2018 Controlling compartmentalization by non-membrane-bound organelles. *Phil. Trans. R. Soc. B* **373**, 20170193. (doi:10.1098/rstb.2017.0193)
- Elbaum-Garfinkle S, Kim Y, Szczepaniak K, Chen CC-H, Eckmann CR, Myong S, Brangwynne CP. 2015 The disordered P granule protein LAF-1 drives phase separation into droplets with tunable viscosity and dynamics. *Proc. Natl Acad. Sci. USA* **112**, 7189–7194. (doi:10.1073/pnas.1504822112)
- Brangwynne CP, Mitchison TJ, Hyman AA, Source DG. 2011 Active liquid-like behavior of nucleoli determines their size and shape in *Xenopus laevis*. *Proc. Natl Acad. Sci. USA* **108**, 4334–4339. (doi:10.1073/pnas.1017150108)
- Nott TJ et al. 2015 Phase transition of a disordered nuage protein generates environmentally responsive membraneless organelles. *Mol. Cell* **57**, 936–947. (doi:10.1016/j.molcel.2015.01.013)
- Brangwynne CP, Eckmann CR, Courson DS, Rybarska A, Hoege C, Gharakhani J, Jülicher F, Hyman AA. 2009 Germline P granules are liquid droplets that localize by controlled dissolution/condensation. *Science* **324**, 1729–1732. (doi:10.1126/science.1172046)
- Kaiser TE, Intine RV, Dunder M. 2008 De novo formation of a subnuclear body. *Science* **322**, 1713–1717. (doi:10.1126/science.1165216)
- Shorter J. 2016 Membraneless organelles: phasing in and out. *Nat. Chem.* **8**, 528–530. (doi:10.1038/nchem.2534)
- Oldfield CJ, Dunker AK. 2014 Intrinsically disordered proteins and intrinsically disordered protein regions. *Annu. Rev. Biochem.* **83**, 553–584. (doi:10.1146/annurev-biochem-072711-164947)
- Uversky VN. 2017 Intrinsically disordered proteins in overcrowded milieu: membrane-less organelles, phase separation, and intrinsic disorder. *Curr. Opin. Struct. Biol.* **44**, 18–30. (doi:10.1016/j.sbi.2016.10.015)
- Anderson P, Kedersha N. 2008 Stress granules: the Tao of RNA triage. *Trends Biochem. Sci.* **33**, 141–150. (doi:10.1016/j.tibs.2007.12.003)
- Zhao H, French JB, Fang Y, Benkovic SJ. 2013 The purinosome, a multi-protein complex involved in the de novo biosynthesis of purines in humans. *Chem. Commun.* **49**, 4444–4452. (doi:10.1039/c3cc41437j)
- French JB et al. 2016 Spatial colocalization and functional link of purinosomes with mitochondria. *Science* **351**, 733–737. (doi:10.1126/science.aac6054)
- Ellis RJ. 2001 Macromolecular crowding: obvious but underappreciated. *Trends Biochem. Sci.* **26**, 597–604. (doi:10.1016/S0968-0004(01)01938-7)
- Dix JA, Verkman AS. 2008 Crowding effects on diffusion in solutions and cells. *Annu. Rev. Biophys.* **37**, 247–263. (doi:10.1146/annurev.biophys.37.032807.125824)
- Luby-Phelps K. 2013 The physical chemistry of cytoplasm and its influence on cell function: an update. *Mol. Biol. Cell* **24**, 2593–2596. (doi:10.1091/mbc.E12-08-0617)
- Zimmerman SB, Trach SO. 1991 Estimation of macromolecule concentrations and excluded volume effects for the cytoplasm of *Escherichia coli*. *J. Mol. Biol.* **222**, 599–620. (doi:10.1016/0022-2836(91)90499-V)
- Jun SK, Yethiraj A. 2009 Effect of macromolecular crowding on reaction rates: a computational and theoretical study. *Biophys. J.* **96**, 1333–1340. (doi:10.1016/j.bpj.2008.11.030)
- Hansen MMK, Meijer LHH, Spruijt E, Maas RJM, Rosquelles MV, Groen J, Heus HA, Huck WTS. 2015 Macromolecular crowding creates heterogeneous environments of gene expression in picolitre droplets. *Nat. Nanotechnol.* **11**, 1–8. (doi:10.1038/nnano.2015.243)
- Dupuis NF, Holmstrom ED, Nesbitt DJ. 2014 Molecular-crowding effects on single-molecule RNA folding/unfolding thermodynamics and kinetics. *Proc. Natl Acad. Sci. USA* **111**, 8464–8469. (doi:10.1073/pnas.1316039111)
- Brooks DE, Sharp KA, Fisher D. 1985 Theoretical aspects of partitioning. In *Partitioning in aqueous two-phase system* (eds H Walter, DE Brooks, D Fisher), pp. 11–84. Orlando, FL: Academic Press.
- Albertsson P-Å. 1970 Partition of cell particles and macromolecules in polymer two-phase systems. *Adv. Protein Chem.* **24**, 309–341. (doi:10.1016/S0065-3233(08)60244-2)

44. Helfrich MR, Mangeney-Slavin LK, Long MS, Djoko KY, Keating CD. 2002 Aqueous phase separation in giant vesicles. *J. Am. Chem. Soc.* **124**, 13 374–13 375. (doi:10.1021/ja028157+)
45. Chang LW, Lytle TK, Radhakrishna M, Madinya JJ, Véléz J, Sing CE, Perry SL. 2017 Sequence and entropy-based control of complex coacervates. *Nat. Commun.* **8**, 1273. (doi:10.1038/s41467-017-01249-1)
46. Piculle L, Lindman B. 1992 Association and segregation in aqueous polymer/polymer, polymer surfactant, and surfactant surfactant mixtures—similarities and differences. *Adv. Colloid Interface Sci.* **41**, 149–178. (doi:10.1016/0001-8686(92)80011-L)
47. Albertsson P-Å. 1985 History of aqueous polymer two-phase partition. In *Partitioning in aqueous two-phase system* (eds H Walter, DE Brooks, D Fisher), pp. 1–10. Orlando, FL: Academic Press.
48. Baskir JN, Hatton TA, Suter UW. 1989 Protein partitioning in two-phase aqueous polymer systems. *Biotechnol. Bioeng.* **34**, 541–558. (doi:10.1002/bit.260340414)
49. Flory PJ. 1953 *Principles of polymer chemistry*. Ithaca, NY: Cornell University Press.
50. Johansson HO, Karlström G, Tjerneld F, Haynes CA. 1998 Driving forces for phase separation and partitioning in aqueous two-phase systems. *J. Chromatogr. B. Biomed. Sci. Appl.* **711**, 3–17. (doi:10.1016/S0378-4347(97)00585-9)
51. Keating CD. 2012 Aqueous phase separation as a possible route to compartmentalization of biological molecules. *Acc. Chem. Res.* **45**, 2114–2124. (doi:10.1021/ar200294y)
52. Iqbal M *et al.* 2016 Aqueous two-phase system (ATPS): an overview and advances in its applications. *Biol. Proced. Online* **18**, 1–18. (doi:10.1186/s12575-016-0048-8)
53. Walter H, Brooks DE, Fisher D (eds). 1985 *Partitioning in aqueous two-phase systems: theory, methods, uses, and applications to biotechnology*. Orlando, FL: Academic Press.
54. Shanbhag VP, Axelsson CG. 1975 Hydrophobic interaction determined by partition in aqueous two-phase systems: partition of proteins in systems containing fatty-acid esters of poly(ethylene glycol). *Eur. J. Biochem.* **60**, 17–22. (doi:10.1111/j.1432-1033.1975.tb20970.x)
55. Albertsson P-Å. 1978 Partition between polymer phases. *J. Chromatogr. A* **159**, 111–122. (doi:10.1016/S0021-9673(00)98551-0)
56. Long MS, Keating CD. 2006 Nanoparticle conjugation increases protein partitioning in aqueous two-phase systems. *Anal. Chem.* **78**, 379–386. (doi:10.1021/ac051882t)
57. Strulson CA, Molden RC, Keating CD, Bevilacqua PC. 2012 RNA catalysis through compartmentalization. *Nat. Chem.* **4**, 941–946. (doi:10.1038/nchem.1466)
58. Huddleston J, Veide A, Köhler K, Flanagan J, Enfors SO, Lyddiatt A. 1991 The molecular basis of partitioning in aqueous two-phase systems. *Trends Biotechnol.* **9**, 381–388. (doi:10.1016/0167-7799(91)90130-A)
59. Ananthapadmanabhan KP, Goddard ED. 1987 Aqueous biphasic formation in polyethylene oxide–inorganic salt systems. *Langmuir* **3**, 25–31. (doi:10.1021/la00073a005)
60. Berggren K, Johansson HO, Yjerneld F. 1995 Effects of salts and the surface hydrophobicity of proteins on partitioning in aqueous two-phase systems containing thermoseparating ethylene oxide–propylene oxide copolymers. *J. Chromatogr. A* **718**, 67–79. (doi:10.1016/0021-9673(95)00657-5)
61. Rito-Palomares M. 2004 Practical application of aqueous two-phase partition to process development for the recovery of biological products. *J. Chromatogr. B* **807**, 3–11. (doi:10.1016/j.jchromb.2004.01.008)
62. Asenjo JA, Andrews BA. 2011 Aqueous two-phase systems for protein separation: a perspective. *J. Chromatogr. A* **1218**, 8826–8835. (doi:10.1016/j.chroma.2011.06.051)
63. Huddleston JG, Willauer HD, Griffin ST, Rogers RD. 1999 Aqueous polymeric solutions as environmentally benign liquid/liquid extraction media. *Ind. Eng. Chem. Res.* **38**, 2523–2539. (doi:10.1021/ie980505m)
64. Burgess DJ. 1994 Complex coacervation: microcapsule formation. In *Macromolecular complexes in chemistry and biology* (eds P Dubin, J Bock, R Davis, DN Schulz, C Thies), pp. 285–300. Berlin, Germany: Springer.
65. Sing CE. 2017 Development of the modern theory of polymeric complex coacervation. *Adv. Colloid Interface Sci.* **239**, 2–16. (doi:10.1016/j.cis.2016.04.004)
66. Koga S, Williams DS, Perriman AW, Mann S. 2011 Peptide-nucleotide microdroplets as a step towards a membrane-free protocell model. *Nat. Chem.* **3**, 720–724. (doi:10.1038/nchem.1110)
67. Aumiller WM, Cakmak FP, Davis BW, Keating CD. 2016 RNA-based coacervates as a model for membraneless organelles: formation, properties, and interfacial liposome assembly. *Langmuir* **32**, 10 042–10 053. (doi:10.1021/acs.langmuir.6b02499)
68. Aumiller WM, Keating CD. 2017 Experimental models for dynamic compartmentalization of biomolecules in liquid organelles: reversible formation and partitioning in aqueous biphasic systems. *Adv. Colloid Interface Sci.* **239**, 75–87. (doi:10.1016/j.cis.2016.06.011)
69. Bungenberg de Jong HG, Kruyt HR. 1929 Coacervation (partial miscibility in colloid systems). *Proc. Acad. Sci. Amsterdam* **32**, 849–856.
70. Overbeek JTG, Voorn MJ. 1957 Phase separation in polyelectrolyte solutions. Theory of complex coacervation. *J. Cell. Comp. Physiol.* **49**, 7–26. (doi:10.1002/jcp.1030490404)
71. Deng NN, Huck WTS. 2017 Microfluidic formation of monodisperse coacervate organelles in liposomes. *Angew. Chemie Int. Ed.* **56**, 9736–9740. (doi:10.1002/anie.201703145)
72. Marianelli AM, Miller BM, Keating CD. 2018 Impact of macromolecular crowding on RNA/spermine complex coacervation and oligonucleotide compartmentalization. *Soft Matter* **14**, 368–378. (doi:10.1039/C7SM02146A)
73. Chollakup R, Smitthipong W, Eisenbach CD, Tirrell M. 2010 Phase behavior and coacervation of aqueous poly(acrylic acid)–poly(allylamine) solutions. *Macromolecules* **43**, 2518–2528. (doi:10.1021/ma902144k)
74. Chollakup R, Beck JB, Dirnberger K, Tirrell M, Eisenbach CD. 2013 Polyelectrolyte molecular weight and salt effects on the phase behavior and coacervation of aqueous solutions of poly(acrylic acid) sodium salt and poly(allylamine) hydrochloride. *Macromolecules* **46**, 2376–2390. (doi:10.1021/ma202172q)
75. Perry SL, Li Y, Priftis D, Leon L, Tirrell M. 2014 The effect of salt on the complex coacervation of vinyl polyelectrolytes. *Polymers* **6**, 1756–1772. (doi:10.3390/polym6061756)
76. Blocher WC, Perry SL. 2017 Complex coacervate-based materials for biomedicine. *Wiley Interdiscip. Rev. Nanomed. Nanobiotechnol.* **9**, 76–78. (doi:10.1002/wnan.1442)
77. Spruijt E, Westphal AH, Borst JW, Cohen Stuart MA, Van Der Gucht J. 2010 Binodal compositions of polyelectrolyte complexes. *Macromolecules* **43**, 6476–6484. (doi:10.1021/ma101031t)
78. Priftis D, Tirrell M. 2012 Phase behaviour and complex coacervation of aqueous polypeptide solutions. *Soft Matter* **8**, 9396–9405. (doi:10.1039/C2SM25604E)
79. Krishna Kumar R, Harniman RL, Patil AJ, Mann S. 2016 Self-transformation and structural reconfiguration in coacervate-based protocells. *Chem. Sci.* **7**, 5879–5887. (doi:10.1039/C6SC00205F)
80. Li L, Srivastava S, Andreev M, Marciel AB, De Pablo JJ, Tirrell MV. 2018 Phase behavior and salt partitioning in polyelectrolyte complex coacervates. *Macromolecules* **51**, 2988–2995. (doi:10.1021/acs.macromol.8b00238)
81. Viereggs JR, Lueckheide M, Marciel AB, Leon L, Bologna AJ, Rivera JR, Tirrell MV. 2018 Oligonucleotide-peptide complexes: phase control by hybridization. *J. Am. Chem. Soc.* **140**, 1632–1638. (doi:10.1021/jacs.7b03567)
82. Quiroz FG, Chilkoti A. 2015 Sequence heuristics to encode phase behaviour in intrinsically disordered protein polymers. *Nat. Mater.* **14**, 1164–1171. (doi:10.1038/nmat4418)
83. Kitadai N, Maruyama S. 2017 Origins of building blocks of life: a review. *Geosci. Front.* **9**, 1117–1153. (doi:10.1016/j.gsf.2017.07.007)
84. Robertson MP, Joyce GF. 2012 The origins of the RNA world. *Cold Spring Harb. Perspect. Biol.* **4**, 1–22. (doi:10.1101/cshperspect.a003608)
85. Pressman A, Blanco C, Chen IA. 2015 The RNA world as a model system to study the origin of life. *Curr. Biol.* **25**, R953–R963. (doi:10.1016/j.cub.2015.06.016)
86. Oparin AI. 1957 *The origin of life on the earth*. New York, NY: Academic Press.
87. Poudyal RR, Cakmak FP, Keating CD, Bevilacqua PC. 2018 Physical principles and extant biology reveal



- roles for RNA-containing membraneless compartments in origins of life chemistry. *Biochemistry* **57**, 2509–2519. (doi:10.1021/acs.biochem.8b00081)
88. Aumiller WM, Davis BW, Hashemian N, Maranas C, Armaou A, Keating CD. 2014 Coupled enzyme reactions performed in heterogeneous reaction media: experiments and modeling for glucose oxidase and horseradish peroxidase in a PEG/citrate aqueous two-phase system. *J. Phys. Chem. B* **118**, 2506–2517. (doi:10.1021/jp501126v)
  89. Martin N, Li M, Mann S. 2016 Selective uptake and refolding of globular proteins in coacervate microdroplets. *Langmuir* **32**, 5881–5889. (doi:10.1021/acs.langmuir.6b01271)
  90. Esquena J. 2016 Water-in-water (W/W) emulsions. *Curr. Opin. Colloid Interface Sci.* **25**, 109–119. (doi:10.1016/j.cocis.2016.09.010)
  91. Shah RK *et al.* 2008 Designer emulsions using microfluidics. *Mater. Today* **11**, 18–27. (doi:10.1016/S1369-7021(08)70053-1)
  92. Utada AS, Fernandez-Nieves A, Stone HA, Weitz DA. 2007 Dripping to jetting transitions in coflowing liquid streams. *Phys. Rev. Lett.* **99**, 094502. (doi:10.1103/PhysRevLett.99.094502)
  93. Whitesides GM. 2006 The origins and the future of microfluidics. *Nature* **442**, 368–373. (doi:10.1038/nature05058)
  94. Baret J-C. 2012 Surfactants in droplet-based microfluidics. *Lab. Chip* **12**, 422–433. (doi:10.1039/C1LC20582J)
  95. Shang L, Cheng Y, Zhao Y. 2017 Emerging droplet microfluidics. *Chem. Rev.* **117**, 7964–8040. (doi:10.1021/acs.chemrev.6b00848)
  96. Hardt S, Hahn T. 2012 Microfluidics with aqueous two-phase systems. *Lab. Chip* **12**, 434–442. (doi:10.1039/C1LC20569B)
  97. Martino C, DeMello AJ. 2016 Droplet-based microfluidics for artificial cell generation: a brief review. *Interface Focus* **6**, 20160011. (doi:10.1098/rsfs.2016.0011)
  98. Song Y, Sauret A, Shum HC. 2013 All-aqueous multiphase microfluidics. *Biomicrofluidics* **7**, 061301. (doi:10.1063/1.4827916)
  99. Cacace DN, Keating CD. 2013 Biocatalyzed mineralization in an aqueous two-phase system: effect of background polymers and enzyme partitioning. *J. Mater. Chem. B* **1**, 1794–1803. (doi:10.1039/C3TB00550J)
  100. Davis BW, Aumiller WM, Hashemian N, An S, Armaou A, Keating CD. 2015 Colocalization and sequential enzyme activity in aqueous biphasic systems: experiments and modeling. *Biophys. J.* **109**, 2182–2194. (doi:10.1016/j.bpj.2015.09.020)
  101. Aumiller WM, Davis BW, Hatzakis E, Keating CD. 2014 Interactions of macromolecular crowding agents and cosolutes with small-molecule substrates: effect on horseradish peroxidase activity with two different substrates. *J. Phys. Chem. B* **118**, 10 624–10 632. (doi:10.1021/jp506594f)
  102. Nott TJ, Craggs TD, Baldwin AJ. 2016 Membraneless organelles can melt nucleic acid duplexes and act as biomolecular filters. *Nat. Chem.* **8**, 569–575. (doi:10.1038/nchem.2519)
  103. Frankel EA, Bevilacqua PC, Keating CD. 2016 Polyamine/nucleotide coacervates provide strong compartmentalization of Mg<sup>2+</sup>, nucleotides, and RNA. *Langmuir* **32**, 2041–2049. (doi:10.1021/acs.langmuir.5b04462)
  104. Tang TYD, van Swaay D, DeMello A, Ross Anderson JL, Mann S. 2015 In vitro gene expression within membrane-free coacervate protocells. *Chem. Commun.* **51**, 11 429–11 432. (doi:10.1039/C5CC04220H)
  105. Crosby J, Treadwell T, Hammerton M, Vasilakis K, Crump MP, Williams DS, Mann S. 2012 Stabilization and enhanced reactivity of actinorhodin polyketide synthase minimal complex in polymer–nucleotide coacervate droplets. *Chem. Commun.* **48**, 11 832–11 834. (doi:10.1039/c2cc36533b)
  106. Aumiller WM, Keating CD. 2016 Phosphorylation-mediated RNA/peptide complex coacervation as a model for intracellular liquid organelles. *Nat. Chem.* **8**, 129–137. (doi:10.1038/nchem.2414)
  107. Nakashima KK, Baaij JF, Spruijt E. 2017 Reversible generation of coacervate droplets in an enzymatic network. *Soft Matter* **14**, 361–367. (doi:10.1039/C7SM01897E)
  108. Wang JT *et al.* 2014 Regulation of RNA granule dynamics by phosphorylation of serine-rich, intrinsically disordered proteins in *C. elegans*. *Elife* **3**, e04591. (doi:10.7554/eLife.04591)
  109. Soares RRG, Silva DFC, Fernandes P, Azevedo AM, Chu V, Conde JP, Aires-Barros MR. 2016 Miniaturization of aqueous two-phase extraction for biological applications: from micro-tubes to microchannels. *Biotechnol. J.* **11**, 1498–1512. (doi:10.1002/biot.201600356)
  110. Ziemecka I, van Steijn V, Koper GJM, Kreutzer MT, van Esch JH. 2011 All-aqueous core-shell droplets produced in a microfluidic device. *Soft Matter* **7**, 9878–9880. (doi:10.1039/c1sm06517c)
  111. Ziemecka I, van Steijn V, Koper GJM, Rosso M, Brizard AM, van Esch JH, Kreutzer MT. 2011 Monodisperse hydrogel microspheres by forced droplet formation in aqueous two-phase systems. *Lab. Chip* **11**, 620–624. (doi:10.1039/C0LC00375A)
  112. Varnell J, Weitz DA. 2012 Microfluidic fabrication of water-in-water (w/w) jets and emulsions. *Biomicrofluidics* **6**, 012808. (doi:10.1063/1.3670365)
  113. Song Y, Shum HC. 2012 Monodisperse w/w/w double emulsion induced by phase separation. *Langmuir* **28**, 12 054–12 059. (doi:10.1021/la3026599)
  114. Moon BU, Abbasi N, Jones SG, Hwang DK, Tsai SSH. 2016 Water-in-water droplets by passive microfluidic flow focusing. *Anal. Chem.* **88**, 3982–3989. (doi:10.1021/acs.analchem.6b00225)
  115. Vanswaay D, Tang TYD, Mann S, DeMello A. 2015 Microfluidic formation of membrane-free aqueous coacervate droplets in water. *Angew. Chemie Int. Ed.* **54**, 8398–8401. (doi:10.1002/anie.201502886)
  116. Papageorgiou DT. 1995 On the breakup of viscous liquid threads. *Phys. Fluids* **7**, 1529–1544. (doi:10.1063/1.868540)
  117. Jia TZ, Hentrich C, Szostak JW. 2014 Rapid RNA exchange in aqueous two-phase system and coacervate droplets. *Orig. Life Evol. Biosph.* **44**, 1–12. (doi:10.1007/s11084-014-9355-8)
  118. Luby-Phelps K. 2000 Cytoarchitecture and physical properties of cytoplasm: volume, viscosity, diffusion, intracellular surface area. *Int. Rev. Cytol.* **192**, 189–221. (doi:10.1016/S0074-7696(08)60527-6)
  119. Torre P, Keating CD, Mansy SS. 2014 Multiphase water-in-oil emulsion droplets for cell-free transcription-translation. *Langmuir* **30**, 5695–5699. (doi:10.1021/la404146g)
  120. Monterroso B, Zorrilla S, Sobrinos-Sanguino M, Keating CD, Rivas G. 2016 Microenvironments created by liquid-liquid phase transition control the dynamic distribution of bacterial division FtsZ protein. *Sci. Rep.* **6**, 35140. (doi:10.1038/srep35140)
  121. Hui Sophia Lee S, Wang P, Kun Yap S, Alan Hatten T, Khan SA. 2012 Tunable spatial heterogeneity in structure and composition within aqueous microfluidic droplets. *Biomicrofluidics* **6**, 1–8. (doi:10.1063/1.3694841)
  122. Sokolova E, Spruijt E, Hansen MMK, Dubuc E, Groen J, Chokkalingam V, Piruska A, Heus HA, Huck WTS. 2013 Enhanced transcription rates in membrane-free protocells formed by coacervation of cell lysate. *Proc. Natl Acad. Sci. USA* **110**, 11 692–11 697. (doi:10.1073/pnas.1222321110)
  123. Sobrinos-Sanguino M, Zorrilla S, Keating CD, Monterroso B, Rivas G. 2017 Encapsulation of a compartmentalized cytoplasm mimic within a lipid membrane by microfluidics. *Chem. Commun.* **53**, 4775–4778. (doi:10.1039/C7CC01289F)
  124. Yasukawa M, Kamio E, Ono T. 2011 Monodisperse water-in-water-in-oil emulsion droplets. *Chem. Phys. Chem.* **12**, 263–266. (doi:10.1002/cphc.201000905)
  125. Kaufman G, Boltyskiy R, Nejati S, Thiam AR, Loewenberg M, Dufresne ER, Osuji CO. 2014 Single-step microfluidic fabrication of soft monodisperse polyelectrolyte microcapsules by interfacial complexation. *Lab. Chip* **14**, 3494–3497. (doi:10.1039/C4LC00482E)
  126. Tice JD, Song H, Lyon AD, Ismagilov RF. 2003 Formation of droplets and mixing in multiphase microfluidics at low values of the Reynolds and the capillary numbers. *Langmuir* **19**, 9127–9133. (doi:10.1021/la030090w)
  127. Yuan H, Ma Q, Song Y, Tang MYH, Chan YK, Shum HC. 2017 Phase-separation-induced formation of Janus droplets based on aqueous two-phase systems. *Macromol. Chem. Phys.* **218**, 1–8. (doi:10.1002/macp.201600422)
  128. Holtze C *et al.* 2008 Biocompatible surfactants for water-in-fluorocarbon emulsions. *Lab. Chip* **8**, 1632–1639. (doi:10.1039/b806706f)
  129. Boreyko JB, Mruetusatorn P, Retterer ST, Collier CP. 2013 Aqueous two-phase microdroplets with reversible phase transitions. *Lab. Chip* **13**, 1295–1301. (doi:10.1039/c3lc41122b)
  130. Zhang Y, Ozdemir P. 2009 Microfluidic DNA amplification—a review. *Anal. Chim. Acta* **638**, 115–125. (doi:10.1016/j.aca.2009.02.038)

131. Morley AA. 2014 Digital PCR: a brief history. *Biomol. Detect. Quantif.* **1**, 1–2. (doi:10.1016/j.bdq.2014.06.001)
132. Vijayakumar K, Gulati S, DeMello AJ, Edel JB. 2010 Rapid cell extraction in aqueous two-phase microdroplet systems. *Chem. Sci.* **1**, 447–452. (doi:10.1039/c0sc00229a)
133. Joensson HN, Andersson Svahn H. 2012 Droplet microfluidics—a tool for single-cell analysis. *Angew. Chemie Int. Ed.* **51**, 12 176–12 192. (doi:10.1002/anie.201200460)
134. Ma S, Thiele J, Liu X, Bai Y, Abell C, Huck WTS. 2012 Fabrication of microgel particles with complex shape via selective polymerization of aqueous two-phase systems. *Small* **8**, 2356–2360. (doi:10.1002/smll.201102715)
135. Roach LS, Song H, Ismagilov RF. 2005 Controlling nonspecific protein adsorption in a plug-based microfluidic system by controlling interfacial chemistry using fluorosurfactants. *Anal. Chem.* **77**, 785–796. (doi:10.1021/ac049061w)
136. Lee A, Tang SKY, Mace CR, Whitesides GM. 2011 Denaturation of proteins by SDS and tetraalkylammonium dodecyl sulfates. *Langmuir* **27**, 11 560–11 574. (doi:10.1021/la201832d)
137. Keating CD, Dominak LM. 2007 Polymer encapsulation within giant lipid vesicles. *Langmuir* **23**, 7148–7154. (doi:10.1021/la063687v)
138. Cacace DN, Rowland AT, Stapleton JJ, Dewey DC, Keating CD. 2015 Aqueous emulsion droplets stabilized by lipid vesicles as microcompartments for biomimetic mineralization. *Langmuir* **31**, 11 329–11 338. (doi:10.1021/acs.langmuir.5b02754)
139. Motta I, Gohlke A, Adrien V, Li F, Gardavot H, Rothman JE, Pincet F. 2015 Formation of giant unilamellar proteo-liposomes by osmotic shock. *Langmuir* **31**, 7091–7099. (doi:10.1021/acs.langmuir.5b01173)
140. Baumgart T, Hunt G, Farkas ER, Webb WW, Feigenson GW. 2007 Fluorescence probe partitioning between Lo/Ld phases in lipid membranes. *Biochim. Biophys. Acta—Biomembr.* **1768**, 2182–2194. (doi:10.1016/j.bbamem.2007.05.012)
141. Menger FM, Angelova MI. 1998 Giant vesicles: imitating the cytological processes of cell membranes. *Acc. Chem. Res.* **31**, 789–797. (doi:10.1021/ar970103v)
142. Long MS, Jones CD, Helfrich MR, Mangelny-Slavin LK, Keating CD. 2005 Dynamic microcompartmentation in synthetic cells. *Proc. Natl Acad. Sci. USA* **102**, 5920–5925. (doi:10.1073/pnas.0409333102)
143. Angelova MI, Dimitrov DS. 1986 Liposome electroformation. *Faraday Discuss. Chem. Soc.* **81**, 303–311. (doi:10.1039/dc9868100303)
144. Andes-Koback M, Keating CD. 2011 Complete budding and asymmetric division of primitive model cells to produce daughter vesicles with different interior and membrane compositions. *J. Am. Chem. Soc.* **133**, 9545–9555. (doi:10.1021/ja202406v)
145. Walde P, Cosentino K, Engel H, Stano P. 2010 Giant vesicles: preparations and applications. *ChemBiochem* **11**, 848–865. (doi:10.1002/cbic.201000010)
146. Méléard P, Bagatolli LA, Pott T. 2009 Giant unilamellar vesicle electroformation. from lipid mixtures to native membranes under physiological conditions. *Methods Enzymol.* **465**, 161–176. (doi:10.1016/S0076-6879(09)65009-6)
147. Li Y, Lipowsky R, Dimova R. 2008 Transition from complete to partial wetting within membrane compartments. *J. Am. Chem. Soc.* **130**, 12 252–12 253. (doi:10.1021/ja8048496)
148. Dimova R, Lipowsky R. 2012 Lipid membranes in contact with aqueous phases of polymer solutions. *Soft Matter* **8**, 6409–6415. (doi:10.1039/c2sm25261a)
149. Dominak LM, Keating CD. 2008 Macromolecular crowding improves polymer encapsulation within giant lipid vesicles. *Langmuir* **24**, 13 565–13 571. (doi:10.1021/la8028403)
150. Dominak LM, Omiatek DM, Gundermann EL, Heien ML, Keating CD. 2010 Polymeric crowding agents improve passive biomacromolecule encapsulation in lipid vesicles. *Langmuir* **26**, 13 195–13 200. (doi:10.1021/la101903r)
151. Dominak LM, Gundermann EL, Keating CD. 2010 Microcompartmentation in artificial cells: pH-induced conformational changes alter protein localization. *Langmuir* **26**, 5697–5705. (doi:10.1021/la903800e)
152. Long MS, Cans AS, Keating CD. 2008 Budding and asymmetric protein microcompartmentation in giant vesicles containing two aqueous phases. *J. Am. Chem. Soc.* **130**, 756–762. (doi:10.1021/ja077439c)
153. Li Y, Kusumaatmaja H, Lipowsky R, Dimova R. 2012 Wetting-induced budding of vesicles in contact with several aqueous phases. *J. Phys. Chem. B* **116**, 1819–1823. (doi:10.1021/jp211850t)
154. Cans AS, Andes-Koback M, Keating CD. 2008 Positioning lipid membrane domains in giant vesicles by micro-organization of aqueous cytoplasm mimic. *J. Am. Chem. Soc.* **130**, 7400–7406. (doi:10.1021/ja710746d)
155. Knoblich JA. 2008 Mechanisms of asymmetric stem cell division. *Cell* **132**, 583–597. (doi:10.1016/j.cell.2008.02.007)
156. Neumüller RA, Knoblich JA. 2009 Dividing cellular asymmetry: asymmetric cell division and its implications for stem cells and cancer. *Genes Dev.* **23**, 2675–2699. (doi:10.1101/gad.1850809)
157. Li Y, Lipowsky R, Dimova R. 2011 Membrane nanotubes induced by aqueous phase separation and stabilized by spontaneous curvature. *Proc. Natl Acad. Sci. USA* **108**, 4731–4736. (doi:10.1073/pnas.1015892108)
158. Dimova R, Lipowsky R. 2017 Giant vesicles exposed to aqueous two-phase systems: membrane wetting, budding processes, and spontaneous tubulation. *Adv. Mater. Interfaces* **4**, 1600451. (doi:10.1002/admi.201600451)
159. Kusumaatmaja H, Li Y, Dimova R, Lipowsky R. 2009 Intrinsic contact angle of aqueous phases at membranes and vesicles. *Phys. Rev. Lett.* **103**, 238103. (doi:10.1103/PhysRevLett.103.238103)
160. van Swaay D, DeMello A. 2013 Microfluidic methods for forming liposomes. *Lab. Chip* **13**, 752–767. (doi:10.1039/c2lc41121k)
161. Karamdad K, Law RV, Seddon JM, Brooks NJ, Ces O. 2015 Preparation and mechanical characterisation of giant unilamellar vesicles by a microfluidic method. *Lab. Chip* **15**, 557–562. (doi:10.1039/C4LC01277A)
162. Shum HC, Lee D, Yoon I, Kodger T, Weitz DA. 2008 Double emulsion templated monodisperse phospholipid vesicles. *Langmuir* **24**, 7651–7653. (doi:10.1021/la801833a)
163. Arriaga LR, Datta SS, Kim SH, Amstad E, Kodger TE, Monroy F, Weitz DA. 2014 Ultrathin shell double emulsion templated giant unilamellar lipid vesicles with controlled microdomain formation. *Small* **10**, 950–956. (doi:10.1002/smll.201301904)
164. Dewey DC, Strulson CA, Cacace DN, Bevilacqua PC, Keating CD. 2014 Bioreactor droplets from liposome-stabilized all-aqueous emulsions. *Nat. Commun.* **5**, 1–9. (doi:10.1038/ncomms5670)
165. Pawar AB, Caggioni M, Ergun R, Hartel RW, Spicer PT. 2011 Arrested coalescence in Pickering emulsions. *Soft Matter* **7**, 7710–7716. (doi:10.1039/c1sm05457k)
166. Balakrishnan G, Nicolai T, Benyahia L, Durand D. 2012 Particles trapped at the droplet interface in water-in-water emulsions. *Langmuir* **28**, 5921–5926. (doi:10.1021/la204825f)
167. Cakmak FP, Keating CD. 2017 Combining catalytic microparticles with droplets formed by phase coexistence: adsorption and activity of natural clays at the aqueous/aqueous interface. *Sci. Rep.* **7**, 3215. (doi:10.1038/s41598-017-03033-z)
168. Peddireddy KR, Nicolai T, Benyahia L, Capron I. 2016 Stabilization of water-in-water emulsions by nanorods. *ACS Macro Lett.* **5**, 283–286. (doi:10.1021/acsmacrolett.5b00953)
169. Tang TYD, Rohaida Che Hak C, Thompson AJ, Kuimova MK, Williams DS, Perriman AW, Mann S. 2014 Fatty acid membrane assembly on coacervate microdroplets as a step towards a hybrid protocell model. *Nat. Chem.* **6**, 527–533. (doi:10.1038/nchem.1921)
170. Brea RJ, Rudd AK, Devaraj NK. 2016 Nonenzymatic biomimetic remodeling of phospholipids in synthetic liposomes. *Proc. Natl Acad. Sci. USA* **113**, 8589–8594. (doi:10.1073/pnas.1605541113)
171. Lagny TJ, Bassereau P. 2015 Bioinspired membrane-based systems for a physical approach of cell organization and dynamics: usefulness and limitations. *Interface Focus* **5**, 20150038. (doi:10.1098/rsfs.2015.0038)
172. Engelhart AE, Adamala KP, Szostak JW. 2016 A simple physical mechanism enables homeostasis in primitive cells. *Nat. Chem.* **8**, 448–453. (doi:10.1038/nchem.2475)
173. Adamala KP, Martin-Alarcon DA, Guthrie-Honea KR, Boyden ES. 2017 Engineering genetic circuit

- interactions within and between synthetic minimal cells. *Nat. Chem.* **9**, 431–439. (doi:10.1038/nchem.2644)
174. Elani Y, Law RV, Ces O. 2014 Vesicle-based artificial cells as chemical microreactors with spatially segregated reaction pathways. *Nat. Commun.* **5**, 5305. (doi:10.1038/ncomms6305)
175. Zhu TF, Szostak JW. 2009 Coupled growth and division of model protocell membranes. *J. Am. Chem. Soc.* **131**, 5705–5713. (doi:10.1021/ja900919c)
176. Adamala K, Szostak JW. 2013 Competition between model protocells driven by an encapsulated catalyst. *Nat. Chem.* **5**, 495–501. (doi:10.1038/nchem.1650)
177. Martos A, Jiménez M, Rivas G, Schwille P. 2012 Towards a bottom-up reconstitution of bacterial cell division. *Trends Cell Biol.* **22**, 634–643. (doi:10.1016/j.tcb.2012.09.003)
178. Jiménez M, Martos A, Cabré EJ, Raso A, Rivas G. 2013 Giant vesicles: a powerful tool to reconstruct bacterial division assemblies in cell-like compartments. *Environ. Microbiol.* **15**, 3158–3168. (doi:10.1111/1462-2920.12214)
179. Wang J *et al.* 2018 A molecular grammar governing the driving forces for phase separation of prion-like RNA binding proteins. *Cell* **174**, 1–12. (doi:10.1016/j.cell.2018.06.006)